ADDIS ABABA UNIVERSITY

SCHOOL OF GRADUATE STUDIES

INTEGRATED GEOPHYSICAL AND DIRECT GEOTECHNICAL INVESTIGATIONS FOR BUILDING FOUNDATION AT ADDIS ABABA SCIENCE AND TECHNOLOGY UNIVERSITY, AKAKI, ADDIS ABABA, ETHIOPIA

BY:

HAILEMARIAM SIYUM

A THESIS SUBMITTED TO THE SCHOOL OF GRADUATE STUDIES OF ADDIS ABABA UNIVERSITY IN PARTIAL FULFILMENT OF THE REQUIREMENTS FOR THE DEGREE OF MASTER OF SCIENCE IN GEOPHYSICS

June, 2011

ADDIS ABABA UNIVERSITY
DEPARTMENT OF EARTH SCIENCE
SCHOOL OF GRADUATE STUDIES

INTEGRATED GEOPHYSICAL AND DIRECT GEOTECHNICAL INVESTIGATIONS FOR BUILDING FOUNDATION AT ADDIS ABABA SCIENCE AND TECHNOLOGY UNIVERSITY, AKAKI, ADDIS ABABA, ETHIOPIA

By:

Hailemariam Siyum

Faculty of science

Department of Earth Sciences

Approved by board of examiners:

Dr. Tigistu Haile Signature ______________

Chairman, Department of Earth sciences

Dr. Tigistu Haile Signature_______________

Advisor

Dr. Abera Alemu Signature______________

Internal Examiner

Dr. Tarun K.Raghuvanshi Signature______________

External Examiner

Declaration

I hereby declare that the work which is being presented in this thesis entitled “Integrated Geophysical and direct Geotechnical investigations for building foundation at Addis Ababa Science and Technology University” is original work of my own, has not been presented for a degree or diploma in any other university and that all source of the material used for the thesis have been duly acknowledged.

Hailemariam siyum Date

(Candidate)

This is to certify that the above declaration made by the candidate is correct to the best of my knowledge.

Dr. Tigistu Haile Date

(Advisor)

Abstract

A foundation study has been conducted on the construction site of the Addis Ababa Science and Technology University Campus. The site is located in the central Ethiopian highlands at the western margin of the Main Ethiopian Rift within the Akaki catchment, locally known as Kilinto. Geophysical techniques have been employed in the work to minimize the problems encountered in relation to the limited number of data points available to spatially describe site conditions; these being the primary factors affecting the accuracy and completeness of any site description. The study is aimed at evaluating the competence and suitability of near surface/shallow depth Earth layers as foundation materials. Geophysical and direct geotechnical methods of investigation were employed in which the electrical resistivity imaging, magnetic, and soils and rocks analysis techniques were respectively used.

The geophysical results revealed that three distinct geoelectrical sequences whose geological interpretations correspond to a topsoil, weathered rock and bedrock. The topsoil is recent sediment deposits, which is composed of dark expansive clay, silty clay/ clayey silt, sandy silt and granular materials. The second layer is highly to completely weathered and fractured scoracious basalt and scoria. The geoelectrical section across the study area shows undulating nature of the bedrock morphology with depth of bedrock beginning from 4 to 20 m. From the combination of electrical imaging and the magnetic survey interpretations, there are evident signatures of fractures/faults within the bedrock which can affect the building foundations in the area. The geotechnical results show that the consistency limits of the soils within the area, have high to very high plasticity, hence, the soils are expected to exhibit high to very high swelling potential.

Overall assessments, the subsoil on or within, where engineering structures will be founded, are not competent for heavy structures. Buildings should preferably be constructed in the southwestern, southern and western part of the study area particularly in the northwestern side of the profile-1and 3 and southeastern side of the Profile-1 where the sediment thicknesses are relatively shallow and with few weak zones.

Acknowledgement

First and foremost I am grateful to my advisor Dr.Tigistu Haile for his help during my field work, fatherly approach, encouragement, crucial comments and sound suggestions that he provided throughout my research work.

I would like to say thanks to Dr.Tarun K.Raghuvanshi and Ato Gebremedhin Berhane (MSc. /Assistant Professor) for providing valuable references and suggestions related with direct geotechnical investigations.

I am also thankful to the Construction Design Share Company where I got the direct geotechnical data and lithological logs of the study area. I am also thankful to the Department of Earth Science for their finance and equipments support that was extended for the present research work.

Last but not the least; I am thankful you to all my family members and friends for their support and encouragement during the period of this work.

Table of Contents **Page No**

List of Figures **Page No**

List of Tables **Page No**

List of Appendices   Page No

Acronym

AASHTO	American Association of State Highway and Transportation Officials
ASTM	American State Testing Materials
CDSC	Construction Design Share Company
BH	Borehole
CPT	Cone Penetration Test
2D	Two dimensional
IAEG	International Association of Engineering Geology
IGRF	International Geomagnetic Reference Field
LL	Liquid Limit
MER	Main Ethiopian Rift
NMC	Natural Moisture Content
RQD	Rock Quality Designation
PI	Plasticity Index
PL	Plastic Limit
PMT	Pressuremeter Test
USCS	Unified Soil Classification System
UTM	Universal Transversal Mercator
VST	Vane Shear Test
SPT	Standard Penetration Test

CHAPTER ONE
INTRODUCTION

1.1 General

One of the basic needs of human beings is shelter in which everything he owns is bounded. These sanctuaries must be safely designed and founded over suitable Earth materials and hence proper foundation is an integral part of a structure. All structures have to be built on soils or rocks. If the foundation studies are not conducted properly it may affect the performance of the structures. The main objective in the study of properties of soil and rock is to lay down certain principles, theories and procedures for the design of a safe and sound structure. The subject of foundation engineering deals with the design of various types of substructures under different soil and environmental conditions. The stability of a structure depends upon the stability of the supporting Earth materials. The important factors that require consideration are the location and depth of foundation. In deciding the location and depth, one has to consider the existence of active faults, failure surfaces, underground cavities, lateral transition of geological formations and ancient remains are some of the most common subjects of concern for construction engineers, besides the geotechnical parameters of the formations. Geophysical methods in cooperation with geotechnical investigations are able to provide answers to those problems, and may even disclose several types of structures that typical geotechnical methods, like drills, or field investigation, might fail to detect (Soupios et al., 2007).

The engineering geological properties of soils and rocks for geotechnical investigations require borings and/or sampling in a close-order grid (Benson, 1993). Yet one commonly accepts data from a limited number of data points to characterize large areas and complex geologic settings. In order to obtain a sufficiently complete picture of site conditions, measurements must be taken over denser spacing than direct sampling in which the geophysical methods can economically provide this denser spacing.

Applied geophysics investigates the physical properties of the ground, providing important information on subsurface material conditions for all types of practical applications. Geophysical investigations are non-intrusive and avoid the disruption that can be caused by drilling, pitting and trenching. A geophysical measurement responds to some change in a physical, electrical or chemical property, such as seismic velocity, density, magnetic, electrical, dielectric, radioactive or thermal. Because of the physical properties of soil and rock are vary widely, one or more of these properties will usually correspond to a geologic discontinuity, such as a stratigraphic contact (i.e. soil and rock) or a structural contact (i.e., a fault). Unlike direct sampling, such as obtaining a soil sample and sending it to a laboratory, each minimum and non-destructive methods responds to a different parameter in a different way.

The applications of geophysical methods are able to investigate and determine soil properties, bedrock depth, topography of the bedrock surface below unconsolidated material, rock type, layer boundaries, water table, weak zones and expansive clays, inhomogeneities of the subsurface, cavities, ancient relics and generally underground structures or bodies that have different physical properties from their geological surroundings (Aubert, 1984; Carrara et al., 2001).

The 2D electrical resistivity imaging and magnetic methods are the most effective methods that can provide a detailed picture of the underground conditions without digging. In many cases, resistivity image surveys can be planned, executed, and the data interpreted in a matter of hours while causing minimum or no impact to the environment. Proper use of resistivity image surveys can provide significant cost saving over other exploratory methods.

1.2 Description of the study area

1.2.1 Location

The study area, the Addis Ababa Science and Technology University, is located in the central Ethiopian highlands at the western edge of the Main Ethiopian Rift. The site is situated southeast of Addis Ababa within the Akaki catchment, at a place locally known as Kilinto, Akaki Kality subcity as shown in Figure 1.1. It is bounded by geographical UTM coordinates of 478500 to 479600 m east and 981700 to 982800 m north.

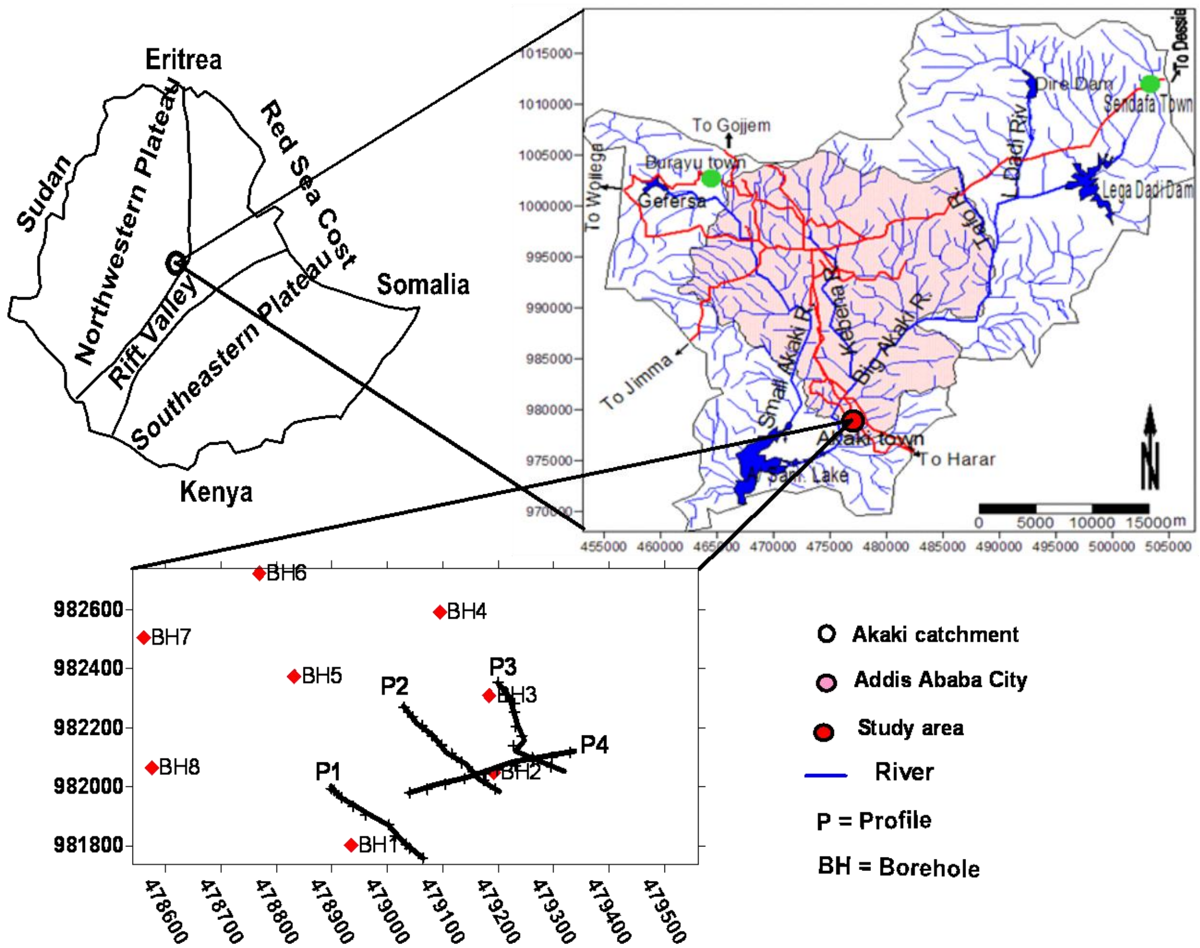

Figure 1.1 Location map of the study area and the geophysical imaging traverses.

1.2.2 Topography

The study area is on a flat to gently sloping topography with small sized erosion gullies crossing it (Figure 1.2). It is currently being utilized for farming. The site is covered by recent deposited sediment of varying thickness.

1.3 Problem Statement

Buildings, like all structures, are designed to support certain loads without deforming excessively. The loads are dead loads, live loads, wind and earthquake forces, lateral pressures exerted by the foundation Earth on the embedded structural elements, and the effects of dynamic loads.

Figure 1.2 Partial view of the site.

The causes of building collapse are bad design, faulty construction, foundation failure, extraordinary loads, unexpected failure modes and combination of causes. Among these factors, foundation failures are mostly related to geotechnical investigation problems.

Before construction of any structure in civil engineering works it requires acquiring information about the geology, engineering properties of soils and rocks, geological structures and hydrogeology of the site. In our country most of the geotechnical investigations are conducted by limited number of boreholes, test pits and trenches. Construction Design Share Company has conducted a direct geotechnical investigation in the study area using a limited number of boreholes. Because of inhemogenity of the material below the Earth's surface, the extrapolation/interpolation of the results obtained from the limited number of tests is not representative results over a larger area. In addition to this, the existence of active faults, failure surfaces, underground cavities, lateral transition of geological formations and ancient remains are difficult to detect from direct geotechnical methods which are important parameters to be considered while designing the building foundations.

Geophysical methods help to resolve the above problems and are capable of producing better extrapolations of `engineering properties of soils and rocks of the whole area below the surface of the Earth by taken denser spacing measurements than direct sampling. These conditions motivate to conduct integrated geophysical and direct geotechnical methods for better understanding of the subsurface properties of Earth layers as foundation material.

1.4 Objectives of the study

General Objective

The main objective of this research is to conduct detail geophysical investigations to image the subsurface geology and to characterize the soils and rocks in terms of their engineering geological properties in view of determining their suitability for building foundation.

Specific Objectives

The Specific objectives of this research are:

- To determine depth to the bedrock and possible depth to water table.
- To determine the depth and thickness of the geological strata and their potential influence on the building foundation.
- To detect lateral and vertical changes and local anomalous geological conditions- lithological contacts and structures- of the site and their influence on engineering structures.
- To map the morphology of the bedrock.
- To classify the soils and rocks of the site in terms of their engineering geological properties and their influence on the building foundation.

1.5 Methodology

The methodology followed in the present research process is based on the objectives formulated in section 1.4. Geophysical and direct geotechnical methods of investigation were employed in which the electrical resistivity imaging, magnetic, and soils and rocks analysis techniques were respectively used. The 2D electrical resistivity and magnetic data were collected along the profiles. The spatial geophysical mapping and modeling has been assisted using software's such as GEOSOFT, RES2DINV, PROSYS–II software and SURFUR 9.11 mainly applied for map interpretation and modeling. The existing geotechnical data collected by Construction Design Share Company were used for this study. The soils of the study area were classified on the basis of their engineering geological properties according to Unified Soil Classification Systems (USCS) and classification proposed by International Association of Engineering Geologists (IAEG, 1981). The generalized Flow chart of methodological approach is described in Figure1.3.

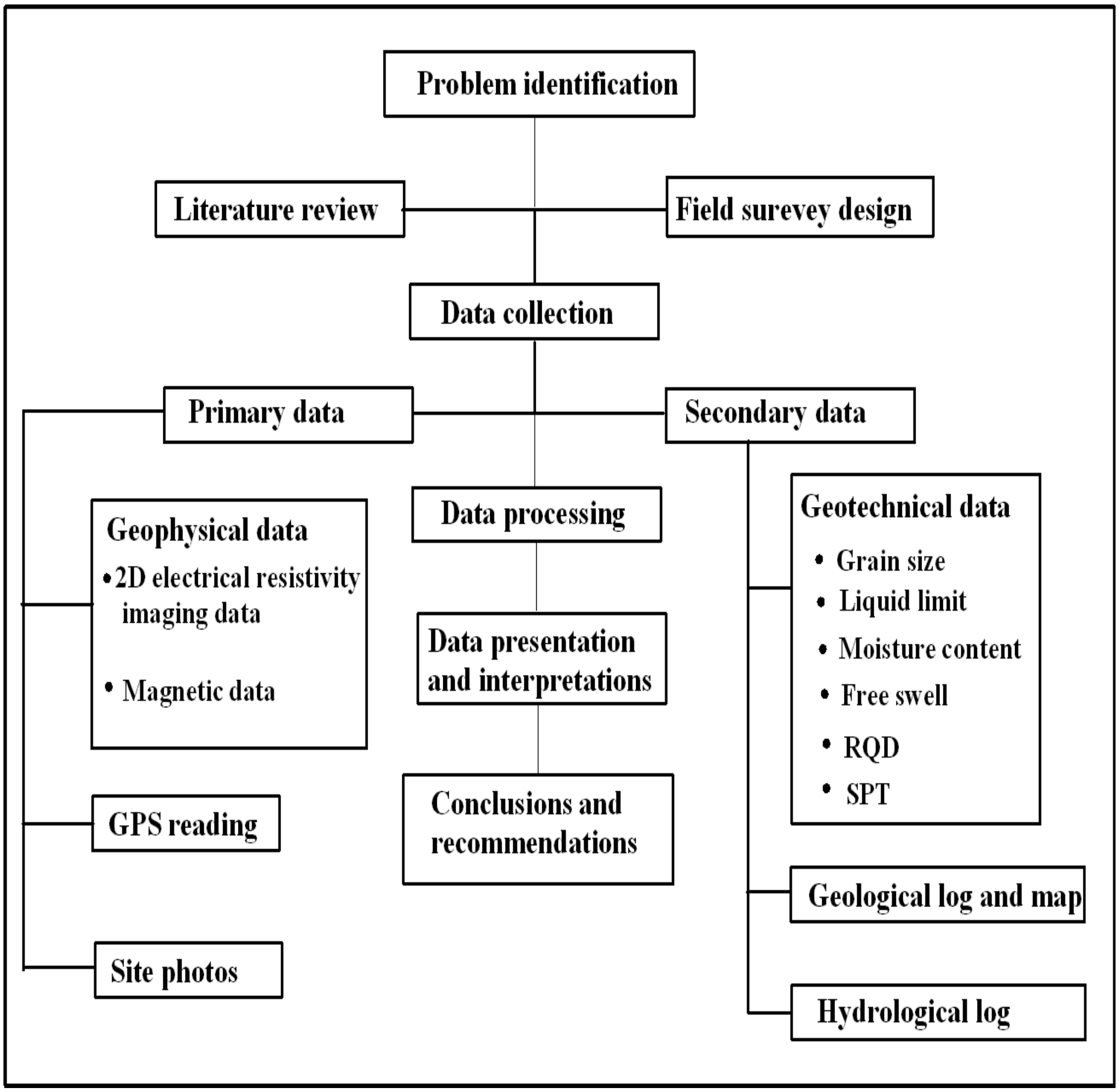

Figure 1.3 Flow chart of methodological approach.

1.6 Previous Works

In the past several geological, hydrogeological, pollution studies and other related works have been performed for different purposes in the study area and its surrounding. The purpose of those studies was mostly concerned with hydrogeological works, to plan and design water supply facilities for the city of Addis Ababa and surrounding towns. A number of works have been done by different scholars. Some of the relevant works are:

1) Haileselassie Girmay and Getaneh Assefa (1989) conducted a systematic study on the geology and volcanic stratigraphic sequences of the Addis Ababa starting from Sululta to Nazareth.
2) Addis Ababa University and Addis Ababa Water and Sewerage Authority (2003) conducted a comprehensive study on groundwater vulnerability mapping of the Addis Ababa area.
3) Ebasa Oljira (2006) conducted a systematic study on the numerical groundwater flow simulation of Akaki river catchment.
4) The Construction Design Share Company (2011) has conducted direct geotechnical investigations to study the engineering properties soils and rocks of the Addis Ababa Science and Technology University. The methods incorporated in this study were drilling of boreholes, Standard penetration test and collections of undisturbed Soil sampling.

1.7 Layout of the Thesis

This thesis is organized in to six chapters. The first chapter is general introduction of the study. The second chapter is concerned mostly with the work of previous researchers that includes geology, hydrogeology and seismicity of the study area and its surrounding. Chapter three covers the theoretical background for the geophysical and direct geotechnical methods employed in this study. Chapter four describes the complete survey procedure, data acquisition, data processing, and presentation of the different results. Chapter five covers integrated results and interpretations of geophysical and direct geotechnical methods. The last chapter contains conclusions and recommendations of the research work.

CHAPTER TWO

GEOLOGY, HYDROGEOLOGY AND SEISMICITY OF THE STUDY AREA

2.1 Geology of the Study Area and its Surrounding

Because of its location at the western margin of the Main Ethiopian Rift (MER), the geological history of the studied area is an integral part of the evolution and development of the Ethiopian Plateau and the Rift system. The area is covered by different volcanic rocks with both acidic and basic compositions and overlain by fluvial and residual soils varying in thickness from a few cm to about 19 m in which black cotton soil is the predominant type (Morton, 1976). Many researchers systematically proposed the geology and volcanic stratigraphic sequences of Addis Ababa area. The geology of Addis Ababa compiled by Haileselassie Girmay and Getaneh Assefa (1989) shows the stratigraphy of the study area and its surrounding. Accordingly, the Miocene-Pleistocene, volcanic successions in the Addis Ababa area from the oldest to the youngest are: Alaji series, Entoto silicics, Addis Ababa basalts, Nazaret group, and Bofa basalts. These are briefly discussed in the following sections. The general geological map of the project area and its surrounding is given in Figure 2.1.

2.1.1 Alaji series

The Alaji group volcanic rocks (Alaji rhyolite and Basalt) are exposed in the Entoto Mountain from the end of Oligocene until middle Miocene (Zanettin and Justin, 1974). This unit is composed of basalts, which show variation in texture from highly pophyric to aphyric. Within this unit there is an intercalation of grey and glassy welded tuff. The outcrop of Alaji basalt extends from the crest of Entoto (ridge bordering the northern parts of Addis Ababa) towards the north (Haileselassie Girmay and Getaneh Assefa, 1989). This unit is underlain by tuffs and ignimbrites.

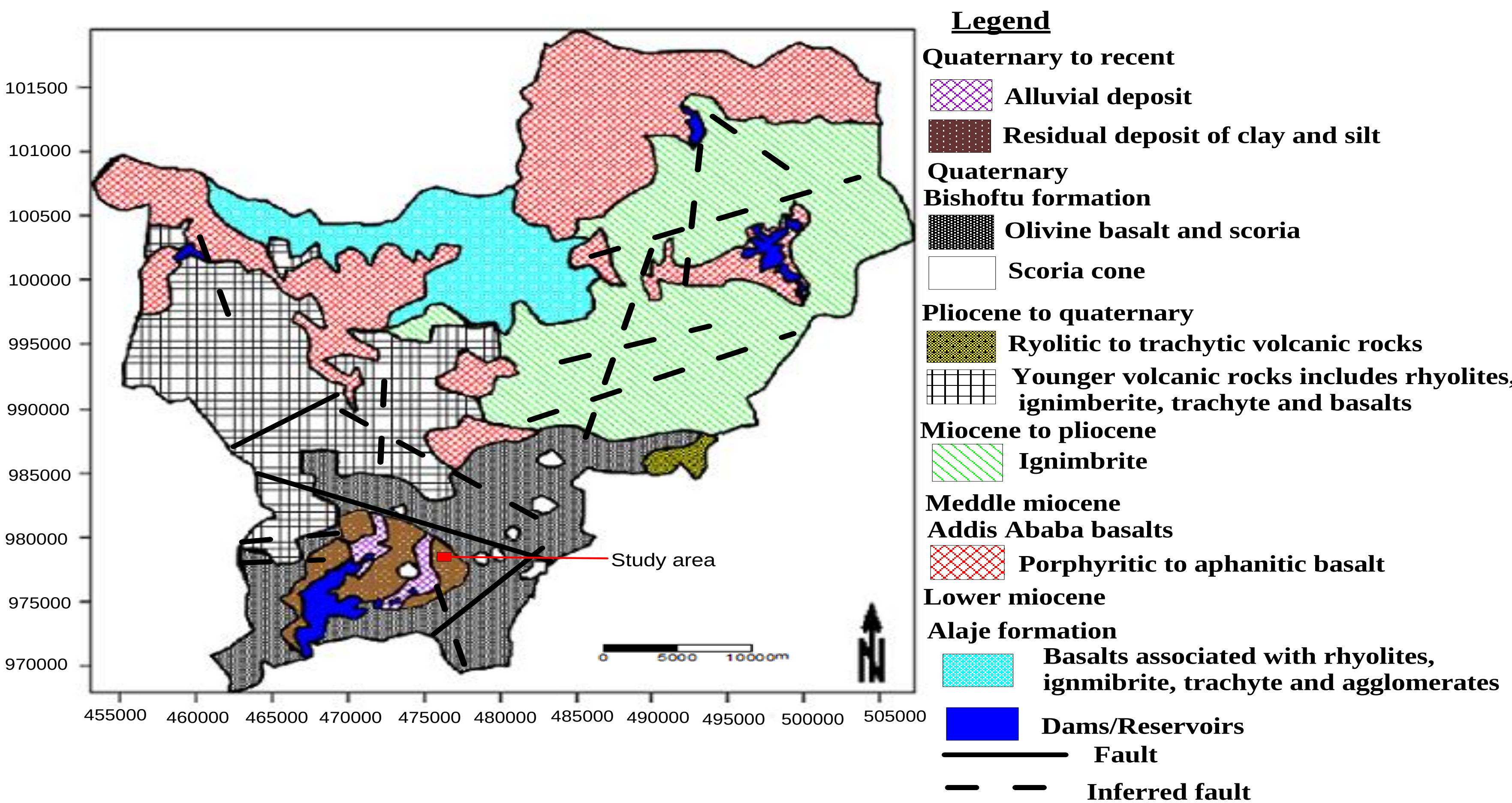

Figure 2.1 Geology of the Akaki catchment in which the study area is found

(after Ebasa Oljira, 2006).

2.1.2 Entoto Silicics

These early Miocene age silicic volcanics could represent localized terminal episodes to massive Oligocene fissure basalt activity in the Addis Ababa region (Morton et al., 1979). The thickness of the flow become maximum on the top of Entoto ridge and thin both towards the plateau and the plain east of Addis Ababa. The unit is unconformably overlain by Addis Ababa basalt on the foothill of Entoto and underlain by Alaji basalt. The Entoto silicics composed of rhyolite and trachyte with minor amount of welded tuff and obsidian (Haileselassie Girmay and Getaneh Assefa, 1989).

2.1.3 Addis Ababa Basalt

This unit, which is mainly present in the central part of the town, is underlain by the Entoto silicics and overlain by Lower welded Tuff of the Nazaret group. The maximum thickness exceeding 130 meters was found at ketchene stream. Olivine porphyritic basalts outcrop in the central part of the town that includes Mercato, Teklehaymanote and Sidist Kilo. The distribution of plagioclase porphyritic basalt is almost the same as that of the olivine prophyritic basalt. It outcrops in an area, which includes Sidist Kilo, General Winget School and French Embassy. The Lower Welded Tuff overlies both types of basalt nearby the Building College, the Kolfe Police School, the Kokobe Tseba School and YecaMariam Church.

2.1.4 Nazaret group

The lithological units identified in this group are Lower Welded Tuff, Aphanitic basalt and Upper Welded Tuff. This group is underlain by Addis Ababa basalt and overlain by Bofa basalts. The rocks outcrop mainly south of Filowha fault and extend towards Nazaret.

Lower Welded Tuff outcrops as small discontinuous body in Filwoha, western parts of Addis Ababa and Sululta. It is glassy with abundant fiamme and has columnar joints. Generally, it is overlain by the aphanitic basalt and underlain by the olivine and plagioclase prophyritic basalt.

Aphanitic Basalt covers the southern part of the town, especially the areas of Bole International Airport and Lideta Airfield. The rock body shows vertical curved columnar jointing together with sub-horizontal sheet jointing. The basalt is overlain by pumeacoues pyroclastic falls and the pyroclastic falls. It consists of Labradorite, augite, rarely olivine and magnetite. The crystals of plagioclase show marked flow alignments.

Upper Welded Tuff outcrops all over the southern part of the town; including Bole, Nefas Silk and Railway station; nevertheless it is also present in the central and northern parts of the town. It is grey colored, vertically and horizontally jointed and composed of sandine, orthoclase, quartz, pumice and unidentified volcanic fragments. The welded tuff is underlain by aphanitic basalts and overlain by young olivine basalts.

2.1.5 Bofa Basalts

This unit comprises of olivine porphyritic basalt, scoria, vesicular & scoriaceous basalt, and trachy - basalt lava flows. They extend in to the south from Akaki River and the unit is as thick as 10 meters (Anteneh Girma, 1994). They appear to have upper thick basalt of 20 - 40m over the Akaki well field but thinner to absent in other places.

2.1.6 Alluvial and Residual Deposits

These are quaternary to recent deposits. Alluvial deposits are found in some places along small and Big Akaki Rivers, especially south and southwest of the capital city. A thick alluvial deposit occurs in the area between Akaki town and Abba Samuel Lake. Some deposits occur along the Kebena River, north-west of Bole area. Soils, which are developed in-situ by the decomposition of rocks, are located in the central, southeast, northeast, Gullele and Kolfe areas. The thickness of these deposits varies between 5m to 50m.

2.2 Geology of the project site

The site is covered by recent sediment deposits, mainly black cotton clay and silt soils. The soil development in the study area is mostly due to the physical disintegration and chemical decomposition of volcanic rocks. The soils in site either remained in place and form residual soils or transported from its surrounding area and deposited in the site area. From the boreholes, the thickness of the sediments varies from place to place and in some places the thickness is greater than 10m. The sediments overlie volcanic rocks. The strata is described below and summarized in tabular form in Appendix-1.

The dark expansive clay soil covers the entire part of the site and is encountered in all boreholes. It is dark, firm to stiff expansive clay and has a thickness ranging from 0.70 to 3.50m. Silty clay/clayey silt are encountered underlying the expansive clay soil in some boreholes. It is stiff, greyish, plastic and has a thickness ranging from 1.10 to 2.50m.

Granular material is the product of intense weathering, fracturing and disintegration of basaltic and scoracious rocks. Mostly, it is greyish or reddish, very dense mixture of gravels, rock fragments, and sometimes core stones. Occasionally, this layer grades into silty sand/sandy silt layer. This layer was encountered only in BH1, BH2, BH3, and BH5 (Appendix-1). It is very dense, greyish or reddish to yellowish, sandy silt. Weathered rocks are encountered at the bottom of all boreholes except in BH2 and BH3. It is greyish, slightly to highly weathered, vesicular (and occasionally massive) basaltic rock with an RQD value ranging from 60% to 100% (CDSC, 2011). Highly weathered and fractured Scoracious rock is also encountered at the site.

2.3 Hydrogeology of the study area

The Occurrence of groundwater in the study area is associated mainly to the volcanic rocks and minor alluvial aquifers that exist along the banks of the main Akaki River and its tributaries. Volcanic rocks, due to their complex spatio-temporal distribution, their different reciprocal stratigraphic relationships, their changeable contacts with ancient and recent rocks, their great compositional, structural and textural variability, and their different level of tectonization and weathering, have complex hydraulic characteristics (Davis and DeWiest, 1966). Like a lot of volcanic terrain in other parts of the world, the hydrogeology of the Akaki catchment is not simple due to the extreme variations of lithology and structure. These Volcanic aquifers have secondary porosities like joints, faults, fractures & fissures produced as a result of tectonic activities where as the alluvial aquifer has primary porosity.

The geometry of the aquifer systems in the catchment area is highly variable, discontinuous and not well defined. In most area, the volcanic aquifers show semi- confined to unconfined nature within few areas (kerchelie and kality), confined aquifers are penetrated. Depth to water level in each well was obtained by subtracting the water level elevation from the ground surface elevation. Based on the borehole data, depth to the water table in the project site is 24m.

2.4 Seismicity of the study area

The important steps in assessment of seismicity are identifying the seismic source zones, distance to the site and geology of the site. The study area is located in the western margin of Main Ethiopia Rift which is tectonically active. Based on the seismicity and the knowledge of the geology and tectonics, the region can be broadly divided into three seismic source zones (Tilahun Mammo, 2005). These are Afar Depression, Escarpment and Ethiopian Rift System seismic source zones which are very near to the study area. The epicenter map of the region in the Figure 2.2 shows that small and intermediate earthquakes are dominated. The location of the earthquake is not uniformly distributed throughout the region, but it is clustering along the Main Ethiopian Rift system. The structural pattern shows that the region is characterized by a complex fault system with orientation almost NE–SW as shown in the Figure 2.3. The geology of the project site is covered by recent loose sediments. The sediments and faults have an ability to amplify the amplitude of the waves. Because of these reasons even small magnitude of earthquake might damage the building structures easily.

Plainly speaking, with the present static knowledge, earthquakes can never be predicted accurately and hence to develop a system warning and eliminating the risk of loss to life is yet a distance dream (Singh, 1997). However, structures in many earthquake prone countries are now being designed more safely.

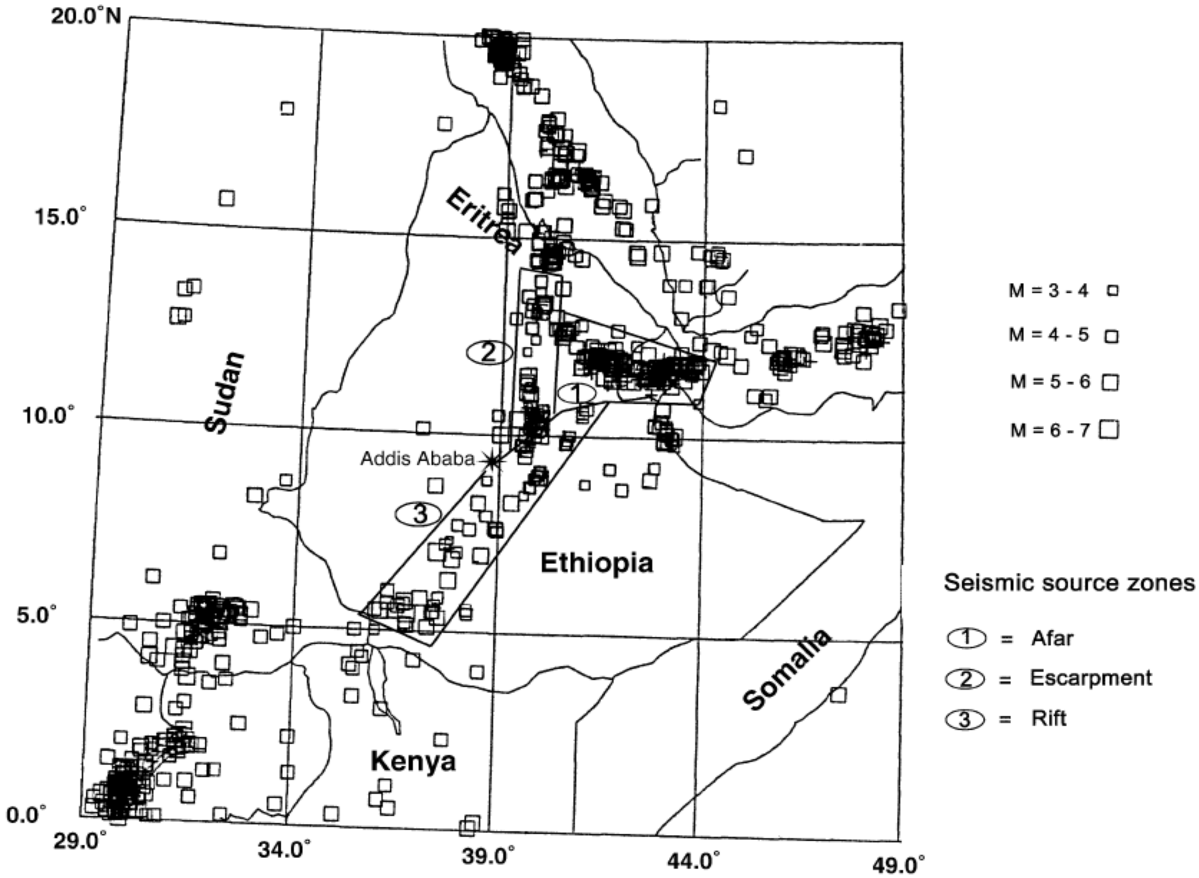

Figure 2.2 Seismicity of the region with the seismic source zones (Tilahun Mammo, 2005).

According to the Ethiopia Building Code Standard (1995), the country is divided into five zones approximately equal seismic risks depending on the known distribution of earthquakes. These zones are no damaging zone (0 zones), less damaging zones (zone 1 and 2) and zones of major damaging (zone 3 and 4). From the seismic hazard map of Ethiopia, the project site falls almost at the boundary of zone two near to the zone three as shown in Figure 2.4. This map is based on the amplitudes of the ground acceleration to be expected during 100 years return period. According to the building code, the ground acceleration ratio (α^{o}) depends on the seismic zones (see Table 2.3 below).

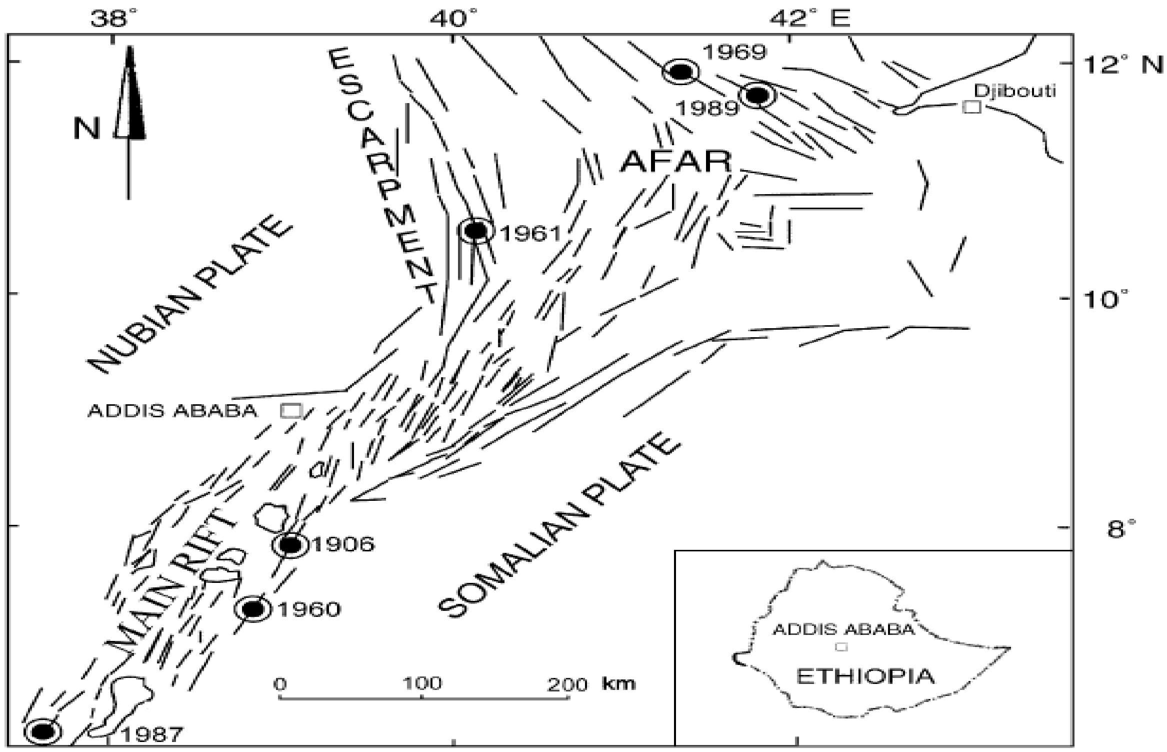

Figure 2.3 Structural pattern of the region and epicenters of the major earthquakes of magnitude above 6.0 (Tilahun Mammo, 2005).

Table 2.1 Bedrock acceleration ratio

Zone	4	3	2	1
α^o	0.10	0.07	0.05	0.03

The ground acceleration value of the project site is 0.05g for 100 year return period. Therefore, the design of Addis Ababa Science and Technology University should include all necessary seismic resistant design parameters.

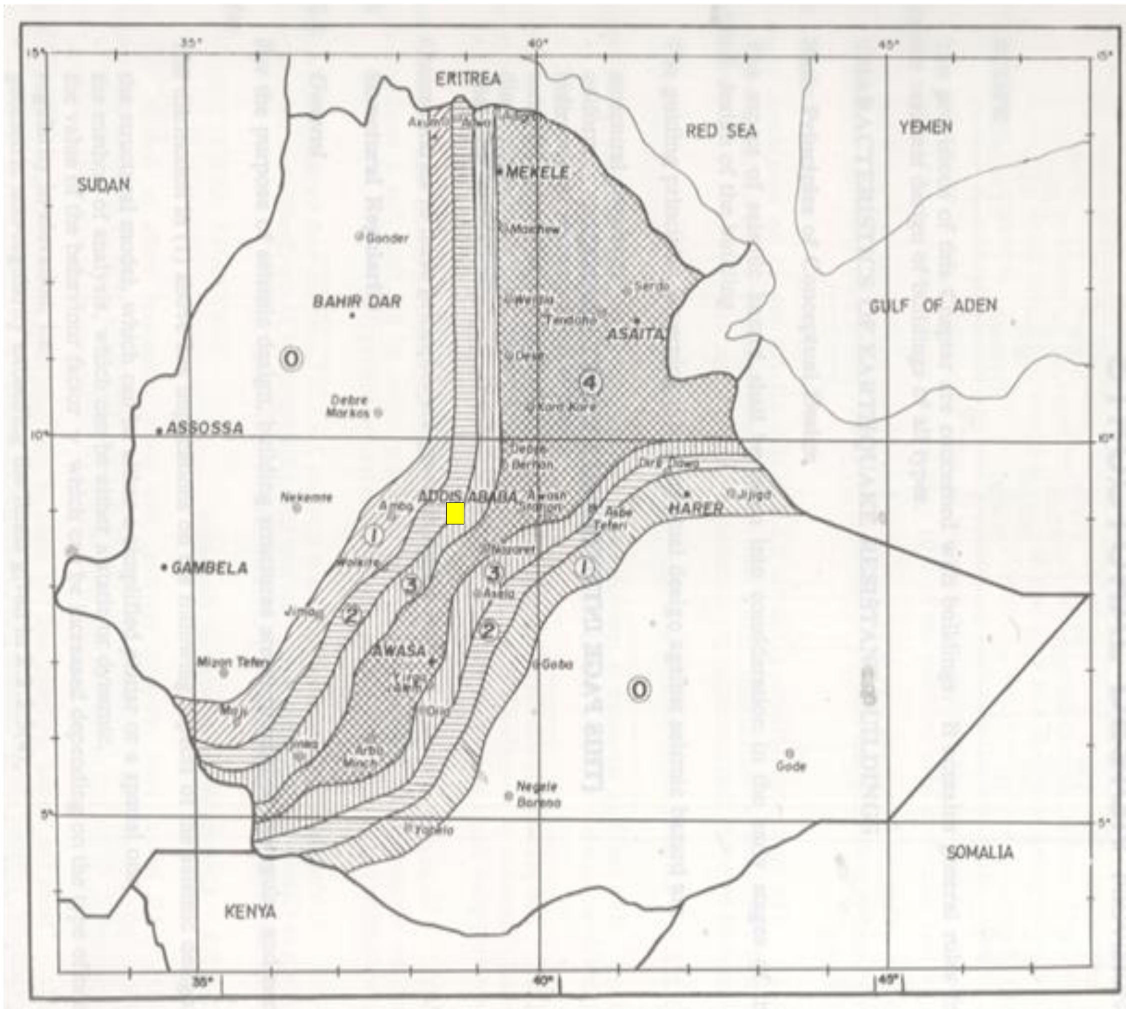

Figure 2.4 Seismic hazard map of Ethiopia (Ethiopian Building Code Standards, 1995) and location of Project area (box).

CHAPTER THREE

THEORETICAL BACKGROUND OF METHODS OF INVESTIGATION

3.1 Direct Current Resistivity Method

3.1.1 Introduction

Electrical resistivity methods were developed in the early 1900s but have become very much more widely used since the 1970s, due to the availability of computers to process and analyze the data. These techniques are used extensively in the search for suitable groundwater sources; in engineering survey to locate subsurface cavities, faults and fissures; in archaeology for mapping the areal extent of remnants of buried foundation of the ancient buildings, amongst many applications (Reynolds, 1997).

The purpose of electrical surveys is to determine the subsurface resistivity distribution by taking measurements on the ground surface. From these measurements, the true resistivity can be estimated. The ground resistivity is related to various geological parameters such as the mineral and fluid content, porosity, nature and degree of water saturation in the rock (Loke, 1999).

3.1.2 Fundamental Principle of DC Resistivity

Electrical resistivity survey is based on the principle that the distribution of electrical potential in the ground around a current-carrying electrode, depends on the electrical resistivities and distribution of the surrounding soils and rocks. The usual practice in the field is to apply an electrical direct current (DC) between the two current electrodes implanted in the ground and to measure the potential difference between the two potential electrodes. If we consider a continuous flow of current in voluminous media, the flow of current in the medium is based on the principles of conservation of energy (Kunetz, 1996).

$$(I_C)_S = -\frac{dQ}{dt} \tag{3.1}$$

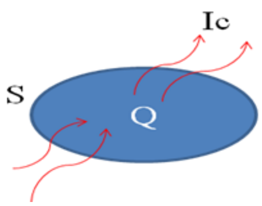

where I_c is the current flowing out of the closed surface '*S*' and '*Q*' is the charge enclosed by '*S*. The current I_c and *Q* can be expressed in terms of the current density (*J*) and the charge density (*q*) as follows.

$$I_C = \oint \vec{J}.ds \quad and \quad Q = \int_V q.dv \tag{3.2}$$

where *v* is the volume bounded by the surface's'. Substituting the equation (3.2) in to the equation (3.1), the equation (3.1) becomes

$$\oint_S \vec{J}.ds = -\frac{d}{dt}\int_v q.dv \tag{3.3}$$

Applying the divergence theorem on the left hand side of the above equation, and interchanging the differentiation and integration sequence on the left hand side of the equation

$$\oint_S \vec{J}.ds = \int_v \left(\nabla.\vec{J}\right)dv \tag{3.4}$$

$$\int_v \left(\nabla.\vec{J}\right)dv = \int_v \left(\frac{\partial q}{\partial t}\right)dv \Leftrightarrow \int_v \left(\nabla.\vec{J} + \frac{\partial q}{\partial t}\right)dv = 0 \tag{3.5}$$

Since equation (3.5) valid for any volume, it can be written as:

$$\nabla.\vec{J} + \frac{\partial q}{\partial t} = 0 \tag{3.6}$$

Equation (3.6) is the law of conservation of charge in differential form, also known as the continuity equation. For stationary value (i.e. direct current) $\partial q/\partial t = 0$ and electric field (*E*) is conservative. The electric field can be expressed as the gradient of scalar potential $\left(E=-\nabla.V\right)$. The Ohm's law can be written in terms of electric field strength (***E***) and current density (***J***) as $J=-\sigma E$, where ***E*** is measured in volts/meter and σ is conductivity. Conductivity is the reciprocal of resistivity (ρ). For isotropic media, ρ is a scalar function of the point of observation and ***J*** is in the same direction as ***E***. Equation (3.6) is reduces to

$$div\left(\frac{1}{\rho}grd.V\right)=grad\frac{1}{\rho}.gradV+\frac{1}{\rho}div.gradV=0 \quad (3.7)$$

This equation is called fundamental equation of electrical prospecting with direct current. For homogenous medium, ρ is independent of the coordinate axes and equation (3.7) is simplified as

$$\nabla^2 V = 0 \quad (3.8)$$

This is called Laplace equation. Therefore, the electrical potential distribution for direct current flow in a homogeneous isotopic medium satisfies the Laplace equation. The Laplace equation has different forms in different coordinate systems as illustrated below.

- Cartesian (orthogonal) coordinate system

$$\frac{\partial^2 V}{\partial x^2}+\frac{\partial^2 V}{\partial y^2}+\frac{\partial^2 V}{\partial z^2}=0 \quad (3.9)$$

- Cylindrical coordinate system

$$\frac{\partial^2 V}{\partial r^2}+\frac{1}{r}\frac{\partial V}{\partial r}+\frac{\partial^2 V}{\partial z^2}+\frac{1}{r^2}\frac{\partial^2 V}{\partial \theta^2}=0 \quad (3.10)$$

- Spherical coordinate system

$$\frac{1}{r^2}\frac{\partial}{\partial r}\left(r^2\frac{\partial V}{\partial r}\right)+\frac{1}{r^2\sin\theta}\frac{\partial}{\partial\theta}\left(\sin\theta\frac{\partial V}{\partial\theta}\right)+ \frac{1}{r^2\sin^2\theta}\frac{\partial^2 V}{\partial\phi^2}=0 \tag{3.11}$$

For hemispherical current distribution, the potential due to single electrode is a function of *r* only, where *r* is the distance from the current source to any equipotential surface. Under these conditions the Laplace equation in the spherical coordinates is our concern. Since, the potential is only as function of *r*; consequently, $\frac{\partial v}{\partial\theta}$ and $\frac{\partial v}{\partial\phi}$ are zero, then equation (3.11) is reduced to

$$\nabla^2 V=\frac{d^2V}{d\,r^2}+\frac{2dV}{rdr}=0 \tag{3.12}$$

Multiplying the equation (3.12) by r^2, then integrating twice both sides of this equation gives

$$V=-\frac{A_0}{r^2}+A_1 \tag{3.13}$$

where, A_0 and A_1 are integration constants and can be solved by using the boundary conditions as follows.

1. Since V= 0 as r $\rightarrow\infty$, then A_1=0
2. $\frac{dV}{dZ}=0$ at Z = 0
3. The current flows radially outwards in all directions from the point electrode. Thus, the total current crossing a hemispherical surface of radius '*r*' is given by I= $2\pi r^2$J, $J=\delta E=-\frac{1}{\rho}\frac{dV}{dr}$ and $\frac{dV}{dr}=\frac{A_0}{r^2}$, so $J=-\frac{1}{\rho}\frac{dV}{dr}$. Substituting these equations in to the equation (3.11) and reduced to

$$V = \frac{I\rho}{2\pi}\left(\frac{1}{r}\right) \tag{3.14}$$

In practice there are always two current electrodes- a positive one through which the current enters to the ground and a negative one to which it returns. Further, we measure potential difference, that is, a voltage difference. In a homogeneous earth, the current flows radially outward from the source to define a hemispherical surface. The current distribution is equal everywhere on this surface which is also called an equipotential surface. Figure 3.1 shows the arrangement of current and potential electrodes, current lines and equipotential surfaces in a homogenous isotropic ground when the direct current source is used.

The goal of resistivity survey is to measure the potential difference between two potential electrodes due to the current from two current electrodes. The potential at each electrode is determined due to the current sources. Suppose that the two current and the two potential electrodes C_1, C_2, and P_1, P_2 respectively are in one line as in Figure 3.1b. C_1 being the positive, C_2 the negative current electrode and k is the geometric factor, then the potential difference is:

$$\Delta V = V_1 - V_2 = I\rho/2\pi\left(1/r_1 - 1/r_2 - 1/r_3 + 1/r_4\right)$$

$$\Delta V = k\frac{I\rho}{2\pi} \tag{3.15}$$

3.1.3 The relationship between geology and resistivity

Resistivity surveys give a picture of the subsurface resistivity distribution. To convert the resistivity picture into a geological picture, some knowledge of typical resistivity values for different types of subsurface materials and the geology of the area surveyed, is important. The resistivity of the geological materials exhibits one of the largest ranges of all physical properties, from 1.6 x $10^{-8}\Omega$m for native silver to $10^{16}\Omega$m for pure sulphur. Igneous and metamorphic rocks typically have high resistivity values.

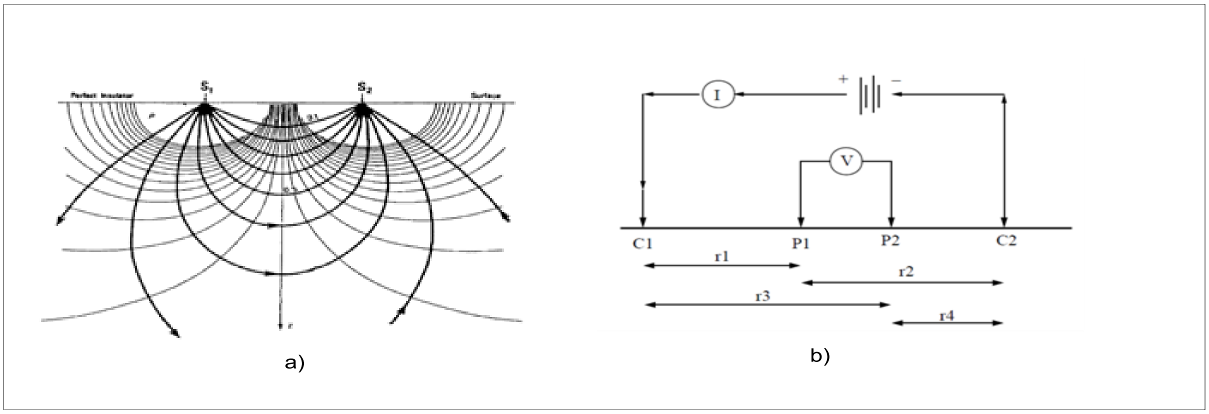

Figure 3.1 a) Current and equipotential lines produced by a current source and sink, b) Generalized form of electrode configuration in resistivity surveys to measure the subsurface resistivity (after Loke, 1997)

The resistivity of these rocks is greatly dependent on the degree of fracturing, and the percentage of the fractures filled with ground water. Sedimentary rocks, which usually are more porous and have higher water content, normally have lower resistivity values. There are overlap of resistivity values of the different classes of rocks and soils. This is because the resistivity of a particular rock or soil sample depends on a number of factors such as the porosity, the degree of water saturation and the concentration of dissolved salts. The resistivity values of common rocks and soil materials (Keller and Frischknecht, 1966; Daniels and Alberty, 1966) are presented in Appendix-2.

3.1.4 2-D electrical imaging survey

3.1.4.1 Introduction

Recently, a new concept of instrumentation and data acquisition has been introduced to make it possible the acquisition of many readings in a reduced amount of time specifically for environmental applications corresponding to shallow investigations depths, of the order of 10 to 80m. The technique is sometimes called Electrical Resistivity Tomography (ERT). The concept involves using multi-core cables which contain as many individual wires as number of electrodes, with one take-out every 5m, 10m … and 24, 48, 72, 96 … electrodes. The measuring unit includes relays which automatically carry out the sequences of readings introduced in its internal memory. The aim of this set-up is to take readings for many combinations of transmission and reception pairs, so as to achieve some kind of mixed wenner / schlumberger array. In such a way of proceeding, the total length of cable is the product of the electrode spacing by the number of electrodes.

The greatest limitation of the resistivity sounding method is that it does not take into account horizontal changes in the subsurface resistivity. A more accurate model of the subsurface is a two-dimensional (2-D) model where the resistivity changes in the vertical direction, as well as in the horizontal direction along the survey line. In this case, it is assumed that resistivity does not change in the direction that is perpendicular to the survey line. In theory, a 3-D resistivity survey and interpretation model should be even more accurate. However, at the present time, 2-D surveys are the most practical economic compromise between obtaining very accurate results and keeping the survey costs down (Loke, 1999).

3.1.4.2 Instrumentation and Field survey

One of the new developments in recent years is the use of 2-D electrical imaging/tomography surveys to map areas with moderately complex geology (Griffiths and Barker, 1993). Such surveys are usually carried out using a large number of electrodes, 25 or more, connected to a multi-core cable. At present, field techniques and equipment to carry out 2-D resistivity surveys are well developed.

Figure 3.2 shows the typical setup for a 2-D survey with a number of electrodes along a straight line attached to a multi-core cable. Normally, a constant spacing between adjacent electrodes is used. The multi-core cable is attached to an electronic switching unit which is connected to a laptop computer. The sequence of measurements to take, the type of array to use and other survey parameters (such the current to use) is normally entered into a text file which can be read by a computer program in a laptop computer. After reading the control file, the computer program then automatically selects the appropriate electrodes for each measurement. One technique used to extend horizontally length covered of the survey, particularly for a system with a limited number of electrodes, is the rollalong method (Figure 3.2). After completing the main sequence of measurements, one of cable is moved to the end of the line.

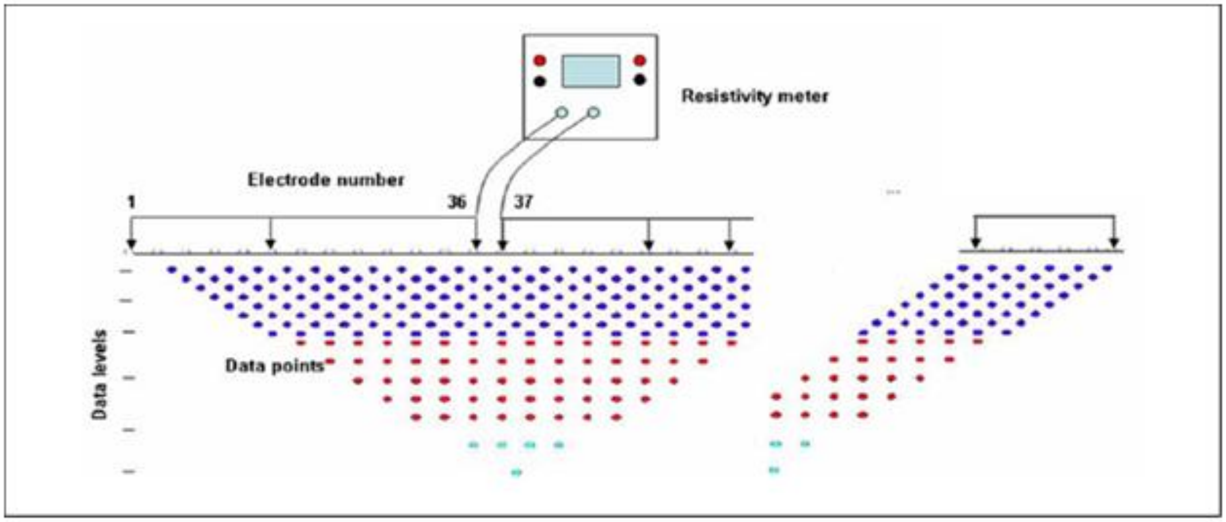

Figure 3.2 Generalized survey procedures with the main sequence in the left, rollalong in the right and data points of 2-D resistivity imaging (Tigistu Haile, 2010).

3.1.4.3 Modeling of 2-D electrical resistivity imaging

Resistivity data is generally interpreted using the modeling process. A hypothetical model of the Earth and its geoelectrical section is generated. The theoretical electrical resistivity response over that model is then calculated. The theoretical response is then comparing with the observed field response and difference between the observed and calculated are noted. The hypothetical earth model is then adjusted to create a response which more fit to the observed data.

a) Forward modeling

Forward modeling is a technique to model a subsurface by estimating the actual resistivity of the different geological structures. The estimation is made by calculating the apparent resistivity of the respective ground structure using the fundamental theoretical electrical equations. The program calculates the apparent resistivity from the recorded current and potential. It then processes and constructs electrical pseudosection of 2-D subsurface model. The forward modeling is achieved by a program that works by dividing the subsurface into a large number of small rectangular cells.

b) Inverse modeling

Geophysical data inversion is a method designed to find a model that gives rise to a parameter similar to the actual measured parameters or data. The model is an idealized mathematical representation of a section of a subsurface earth, having a set of model parameters that are the physical quantities that are estimated from the observed data. The instrument measures the apparent resistivity of the subsurface materials. This is not the true resistivity of the sub surface materials. The relationship between the apparent resistivity and the true resistivity is a complex relationship. The complex mathematical formulation required to determine the true subsurface resistivity from the apparent resistivity values is inversion problem. A program developed to solve this problem is referred to as an inversion program.

The optimization method basically tries to reduce the difference between the calculated and measured apparent resistivity values by adjusting the resistivity of the model blocks. A measure of this difference is given by the root-mean squared (RMS) error. However, the model with the lowest possible RMS error can sometimes show large and unrealistic variations in the model resistivity values and might not always be the "best" model from a geological perspective. In general the most prudent approach is to choose the model at the iteration after which the RMS error does not change significantly. This usually occurs between the 3rd and 5th iterations. The root mean squared (RMS) error equation given as

$$e=\sum_{i=1}^{n}\sqrt{(m_i-r_i)^2} \tag{3.16}$$

where, r_i is the i^{th} calculated (model response) resistivity value, m_i stands for ith observed or input apparent resistivity, n is the number of measured data. In matrix form, taking all r_i and m_i each and their difference (let $g_i = (m_i - r_i)^2$ as column vectors; r, m and g and rearranging the above equation can be formulated for square error function as

$$e = \sum_{i=1}^{n} g^2 = g^T g \tag{3.17}$$

Vector ***g***, that is the difference between the observed and the model response is called discrepancy vector. To get the minimum RMS error the smoothness constrained least-squares method (DeGroot-Hedlin and Constable, 1990; Sasaki 1992) is used. The smoothness-constrained least-squares method is based on the following equation.

$$\left(J^T J + U.F\right)d = J^T g \tag{3.18}$$

where, $F = f_x f_x^T + f_z f_z^T$, f_x = horizontal flatness filter, f_z = vertical flatness filter, J = matrix of partial derivatives, U = damping factor, d = model perturbation factor and g = discrepancy vector.

3.2 Magnetic Method

3.2.1 Introduction

Magnetic prospecting, the oldest method of geophysical exploration, is used for mineral, groundwater, oil and gas, engineering (locating buried structures and weak zones) and environment applications. It is a very popular and inexpensive approach for near-surface metal detection. Engineering and environmental site characterization often begin with a magnetometer survey as a means of rapidly providing a layer of information on where utilities and other buried concerns are located. The principal operation of magnetic survey is quite simple. When a ferrous material is placed within the Earth's magnetic field, it develops an induced magnetic field. The induced field is superimposed on the Earth's field at that location creating a magnetic anomaly. Detection depends on the amount of magnetic material present and its distance from the sensor (Rivas, 2009).

3.2.2 Principles and Elementary Theory

Understanding the magnetic effects associated with Earth materials requires a knowledge of the basic principles of magnetism. In this section review the elementary physical concepts that are fundamental to magnetic prospecting.

If two magnetic poles of strength P_0 and P_1 are separated by a distance *r*, a force (*F*) exists between them. When the poles have the same polarity, the force will push the poles apart, and if they are of opposite polarity, the force is attractive and will draw the poles together. The equation for *F* is obtained from coulomb's law and mathematically given by:

$$F = \frac{1}{\mu} \frac{P_0 P_1}{r^2} \tag{3.19}$$

The constant μ, known as magnetic permeability, depend upon the magnetic properties of the medium in which the poles are situated.

The magnetic field strength at a point is defined as the force per unit of pole strength which would be exerted upon a small pole of strength P_0 if placed at that point. The field strength (*H*) due to a pole of strength (*P*) a distance (r) is

$$H = \frac{F}{P_0} = \frac{P}{\mu r^2} \tag{3.20}$$

A magnetic body is placed in an external magnetic field becomes magnetized by induction. The degree to which the body gets magnetized is proportional to the magnetizing field strength and its direction of the applied magnetic field. Intensity of magnetization is defined as the magnetic moment per unit volume.

$$I = \frac{M}{V} \tag{3.21}$$

where, I is magnetic induction, *M* is magnetic moment, *V* is volume

Magnetic susceptibility (K) is the property of a material which determines how much body is magnetized due to external magnetic field. Magnetic susceptibility is the fundamental parameters in magnetic prospecting. Rocks that have a significant concentration of ferro and/or ferri magnetic minerals tend to have the highest susceptibilities. Consequently basic and ultra basic rocks have the highest susceptibilities, acid igneous and metamorphic rocks have intermediate to low value, and sedimentary rocks have very small susceptibilities. The magnetic susceptibilities of rocks and minerals are explained in the Appendix-2. It is defined as the ratio of intensity of magnetization (I) to the magnetic field strength (H).

$$K = \frac{I}{H} \tag{3.22}$$

The ratio of flux density (B) to magnetic field strength (H) is a constant called absolute magnetic permeability (μ). Practically, the magnetic permeability of water and air can be equal to the magnetic permeability of free space, denoted as μ_0 which has a value of 4µx 10^{-7}Wb/Am for any medium other than a vacuum, the ratio of permeability of a medium to the free space is called relative permeability (μ_r), such that $\mu_r = \mu/\mu_0$

$$B = \mu H \tag{3.23}$$

Since$\mu_r = \mu/\mu_0$ and $k = \mu_r - 1$, then the equation (3.23) becomes

$$B = \mu_0 H + \mu_0 kH = \mu_0 (H + I) \tag{3.24}$$

3.2.3 The Earth's magnetic field

The geomagnetic field at or near the surface of the Earth originates largely from within and around the Earth's core. Ninety percent of the Earth's magnetic field looks like a magnetic field that would be generated from a dipolar magnetic source located at the center of the Earth and aligned with the Earth's rotational axis. The remaining 10% of the magnetic field cannot be explained in terms of simple dipolar sources. As observed on the surface of the earth, the magnetic field can be broken into three separate components.

The main field is the largest component of the magnetic field and is believed to be caused by electrical currents in the Earth's fluid outer core. For exploration work, this field acts as the induced magnetic field. The external magnetic field is a relatively small portion of the observed magnetic field that is generated from magnetic sources external to the earth. This field is believed to be produced by interactions of the Earth's ionosphere with the solar wind. Hence, temporal variations associated with the external magnetic field are correlated to solar activity. The crustal field is the portion of the magnetic field associated with the magnetism of crustal rocks. This portion of the field contains both magnetism caused by induction from the Earth's main magnetic field and remanent magnetization (Thomas, 2003).

3.2.4 Variations of Earth's magnetic field

It was recognized that the Earth's magnetic field changes its direction and intensity with time. These variations resolved in to secular variation, diurnal variation and variations due to magnetic storms. It is clear that the geomagnetic and magnetic poles positions drift with time, known as secular variation in the magnetic field. In addition, the intensity of the main magnetic field is decreasing at about 5% per century. The rate of change, although very significant on a geological time scale, does not affect the data acquisition on a typical exploration survey unless it covers large geographical areas and takes many months to complete.

Diurnal variation is the variation in the magnetic field that occurs over the course of a day and related to variations in the Earth's external magnetic field. These are caused by changes in the strength and direction of the currents in the ionosphere. This variation can be on the order of 20 to 30 nT per day and should be accounted when conducting exploration magnetic surveys.

Occasionally, magnetic activities in the ionosphere unexpectedly increase. The occurrence of such storms correlates with enhanced sunspot activity. The magnetic field observed during such times is highly irregular and unpredictable, having amplitudes as large as 1000 nT. When the magnetic storms occurred, magnetic surveys should be stopping (Lowrie, 2007).

3.2.5 Magnetics Instruments

Magnetometers used specifically in geophysical exploration can be classified into three groups: the torsion, fluxgate and resonance types. Magnetometers measure horizontal and/or vertical components of the magnetic field or the total field. There are two main types of resonance magnetometer: the proton free-precession magnetometer, which is the best known, and the alkali vapour magnetometer. Both types monitor the precession of atomic particles in an ambient magnetic field to provide an absolute measure of the total magnetic field (*F)*. The proton magnetometer has a sensor which consists of a bottle containing a proton-rich liquid, usually water or kerosene, around which a coil is wrapped, connected to the measuring apparatus (Reynolds, 1997).

3.2.6 Field Survey Procedures

Magnetic data can be acquired in two configurations. These are rectangular grid pattern and along a traverse. Grid data consists of readings taken at the nodes of a rectangular grid; traverse data is acquired at fixed intervals along a line. Each configuration has its advantages and disadvantages, which are dependent upon variables such as the site conditions, size and orientation of the target, and financial resources. In both traverse and grid configurations, the station spacing, or distance between magnetic readings, is important.

In the vast majority of the cases where the magnetic targets have a substantial strike length, survey profiles should, where possible, be conducted across strike. In cases such as some archeological and engineering site investigations where the targets are more equidimensional north-south and east-west orientations are commonly used. In ground based surveys, it is important to establish a local base station in an area away from suspected magnetic targets or magnetic noise and where the local field gradient is relatively flat. A base station should be quick and easy to relocate and reoccupy. As the survey progresses, the base station must be re-occupied every half of an hour in order to compile a diurnal variation curve for later correction (Reynolds, 1997).

3.2.7 Magnetic Data Reduction

All magnetic data sets contain elements of noise and will require some form of correction to the raw data to remove all contributions to the observed magnetic fields other than those caused by the sub surface magnetic sources. The most significant correction is for the diurnal variation (δB) in the earth's magnetic field. Base station readings taken over the period of a survey facilitates the compilation of the diurnal variation. Measurements of the total field made at other stations can easily be adjusted by the variation in the diurnal curve. The dipole field (B_d) was determined from international geomagnetic reference field (IGRF) map is subtracted from the measurements at each station to generate magnetic anomalies as:

$$\Delta B = B_{obs} \pm \partial B - B_d \tag{3.25}$$

3.3 Direct subsurface exploration methods and engineering properties of soils and rocks

3.3.1 Introduction

The purpose of this section is to provide information on various direct subsurface explorations, laboratory and in situ testing methods, and classification of soils and rocks. This information helps to establish engineering geological properties of soils and rocks that are important for design of building foundations. The execution of a conventional subsurface exploration and testing program usually includes drilling, pits, trenches, laboratory and in situ testing.

3.3.2 Direct subsurface exploration methods

The most common direct subsurface exploration methods are pits, trenches, and drilling boreholes. The choice for the selection of particular method depends upon the requirements and the type of structure. Pits and trenches are the simplest methods of observing subsurface soils. They consist of excavations performed by hand or dozer. Trenches, to a depth of some 5 m can provide a flexible, rapid and economic method of obtaining information. Pits are expensive and should be considered only if the initial subsurface survey has revealed any areas of special difficulty. The soil conditions in pits and trenches also can be photographed and, undisturbed as well as disturbed, samples can be collected. Most of the detailed geological information during the exploration is obtained by drilling boreholes systematically (Raghuvanshi, 2010). The main purposes of drilling borehole are:

- To established the subsurface distribution of materials with distinctive properties.
- To evaluate engineering geological properties of soils and rocks by collecting samples from each layers.
- To understand the groundwater conditions.
- To provide access for introduction of in-situ testing tools.

3.3.3 Laboratory Tests and In-situ tests

In geotechnical engineering, one needs to determine the range of potential behaviors of a given soil type based on only a few simple tests. Classification and index tests (water content, Atterberg limits, and grain size) should be performed on most or all samples and shear tests should be performed on selected representative undisturbed samples.

The most common in-situ test methods are Standard Penetration Test (SPT), Cone Penetration Test (CPT), Vane Shear Test (VST) and Pressuremeter Test (PMT). Among these methods in this section only standard penetration test is described in detail. The most commonly used in-situ test in the world is the Standard Penetration Test (SPT). The SPT is a simple and rugged test suitable for most soil types except gravel. Many engineers have experience using SPT resistance for design purposes. The test does provide a rough index of the relative strength and compressibility of the soil in the vicinity of the test.

Standard Penetration Test procedures consist of repeatedly dropping a 63.5-kg hammer from a height of 760 mm to drive a split-spoon (i.e., split-barrel) sampler in three successive 150-mm long increments. The numbers of blows required to drive the sampler is recorded for each 150-mm increment. The initial 150-mm increment is considered a seating drive. The blows required for the second and third 150-mm increments are totaled to provide blows/300 mm. This total is referred to as the SPT resistance or “N-value”. Blow counts taken for each 150-mm interval should be recorded, even for the seating increment. The measured N-value is the number of blows required to drive the split spoon sampler a distance of 300 mm (Skempton, 1986).

3.3.4 Descriptions, Index properties and Classification of soils

3.3.4.1 Introduction

The term soil in engineering is defined as unconsolidated material composed of solid particles by disintegration of rocks. Soils are formed from rocks due to chemical, physical and biological weathering. The factors that facilitated the degree of weathering are temperature change, frost action, plant roots and variation of moisture content. When the soil is deposit in-situ after disintegration of the parent rocks, it is called residual soil. On the other hand when the soil is transported and deposited in some places it is a called transport soil.

3.3.4.2 Grain size

Grain size is the size of individual particles in a given soil material. Soils with different grain size have different engineering geological properties. Because of this one should carry out analysis for the proportion of particle size of soils in a given soil sample. Soils are primarily identified as coarse grained, fine grained, and organic soils. On a textural basis, coarse-grained soils are those that have 50 percent or more by weight of the overall soil sample retained on the No. 200 sieve; fine-grained soils are those that have more than 50 percent by weight passing the No. 200 sieve. Highly-organic soils are, in general, readily identified by visual examination. Each soil type gravel, sand, silt and clay is identified by grain size. Based on the diameter or size range adopted from ASTM, soils can be classified as gravel (>4.75 mm); sand (4.75 – 0.075) mm; silt (0.075 – 0.002 mm) and clay (< 0.002 mm).

The results obtained from the sieve and hydrometer analysis are plotted with the percentage of particle size on the y-axis on the arithmetic scale paper and the grain size on the x–axis on the logarithm scale. The shapes of the curves indicate the nature of the soil tested. On the basis of the shapes one can classify soils as: uniformly graded or poorly graded, well graded and gap graded soils. The uniformly graded soils are represented by nearly vertical lines and possess particles of almost the same diameter. A well graded soil, represented by S shape curve possesses a wide range of particle sizes ranging from gravel to clay size particles. A gap graded soil has some of the sizes of soil particles are missing (Holtz and Kovacs, 1981).

3.3.4.3 Atterberg limits and derived index

Atterberg limits are a basic measure of nature of fine grained soils. Depending on the water content of soils; it may appear in four states: solid, semi–solid, plastic and liquid. In each state the consistency and behavior of soils is different and thus so are its engineering properties. The boundary between each state can be defined based on a change in the soil's behavior. The Atterberg limits can be used to distinguish between silt and clay, and it can distinguish between different types of silts and clays.

The values of Atterberg Limits are used in a number of ways. There is also a close relationship between the limits and properties of a soil such as compressibility, permeability, and strength. This is thought to be very useful because limit determination is relatively simple; it is more difficult to determine the other properties like permeability, strength, compressibility etc. The Atterberg Limits are not only used to identify the soil's classification, but it allows for the use of empirical correlations for some other engineering properties (Holtz and Kovacs, 1981).

Liquid limit is defined as the moisture content at which soil begins to behave as a liquid material and begins to flow. In other word it means the lowest water content above which soil behaves like liquid. On the basis of liquid limit plasticity of fine grain soils are classified as shown in the Table 3.1.

Plastic limit is defined as the moisture content at which soil begins to behave as plastic materials. This means it is the lowest water content at which soil behaves like a plastic material. Shrinkage limit is defined as the moisture content at which no further volume change occurs with further reduction in moisture content. The Plasticity Index (PI) is a measure of the plasticity of a soil. The plasticity index is the size of the range of water contents where the soil exhibits plastic properties. The PI is the difference between the liquid limit and the plastic limit (PI = LL-PL). Soils with a high PI tend to be clay, those with a lower PI tend to be silt, and those with a PI of 0 (non-plastic) tend to have little or no silt or clay (Holtz et.al, 1981).

Table 3.1 Classification of plasticity based on the Liquid limit (IAEG, 1981)

Liquid limit (LL) in %	Plasticity
< 35	low plasticity
35 – 50	intermediate plasticity
50 – 70	high plasticity
70 – 90	very high plasticity
>90	extremely high plasticity

Tests used to detect potential problems for coarse grained soils (gravels and sands) are different than those used to detect potential problems for fine grained soils (silts and clays). In case of coarse grained soils water content is generally not a major factor leading to shrinkage of the structure of the soil skeleton. In the fine grain soils water content is a major factor, especially when the soil contains active clay. Because of those fine grained soils are subdivided on the basis of their liquid limit using the plasticity chart as shown in the Figure 3.3. Soils that plot above the A-line are clays and those, which plot below it, are silts. In turn, the plasticity of the soil may be described as low, intermediate, high, very high, or extremely high by reference to the liquid limit.

3.3.4.4 Measurement of potential swell

Many tests and methods have been developed or modified for estimating potential swell. These are direct and indirect measurements. Indirect methods involve the use of soil properties and clay content to estimate swell potential. The change in moisture contents (Atterberg Limits) of a soil sample can be used to indicate the degree for potential swell as presented in Table 3.2. A soil sample with liquid limit exceeding 70% and plasticity index greater than 35% is judged to have a very high potential swell (Holtz and Gibbs, 1956).

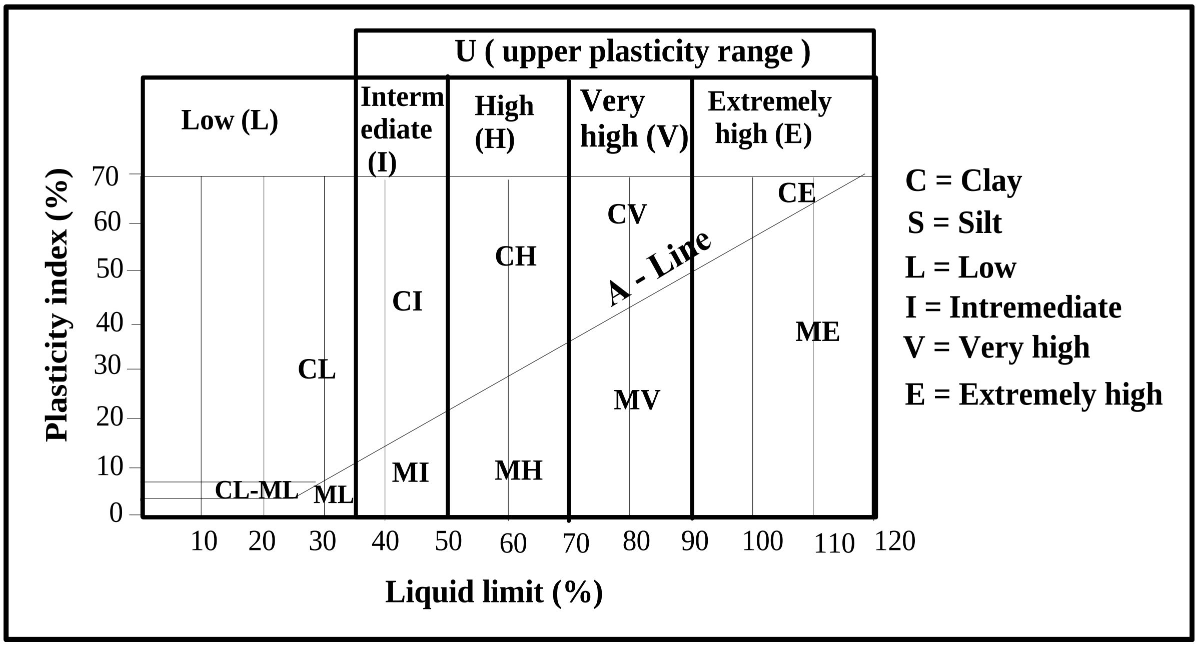

Figure 3.3 Classification of fine grained soils on plasticity chart (IAEG, 1981).

Table 3.2 Classification of potential swell based on plasticity (Holtz and Gibbs, 1956)

Classification of potential swell	Liquid limit (LL),%	Plasticity Index (PI),%	Shrinkage Limit (SL), %
Low	20-35	<18	>15
Medium	35-50	15-28	10-15
High	50-70	25-41	7-12
Very high	>70	>35	<11

Seed et al., (1960); Van der Merwe (1964), and Skempton (1953), established useful empirical relationships between expansion potential and physical properties of soils such as clay contents and soil suction. A preliminary classification based on percentage clay fraction, soil particles less than 2 µm and plasticity index can be used to categorize probable severity as shown in Figure 3.4.

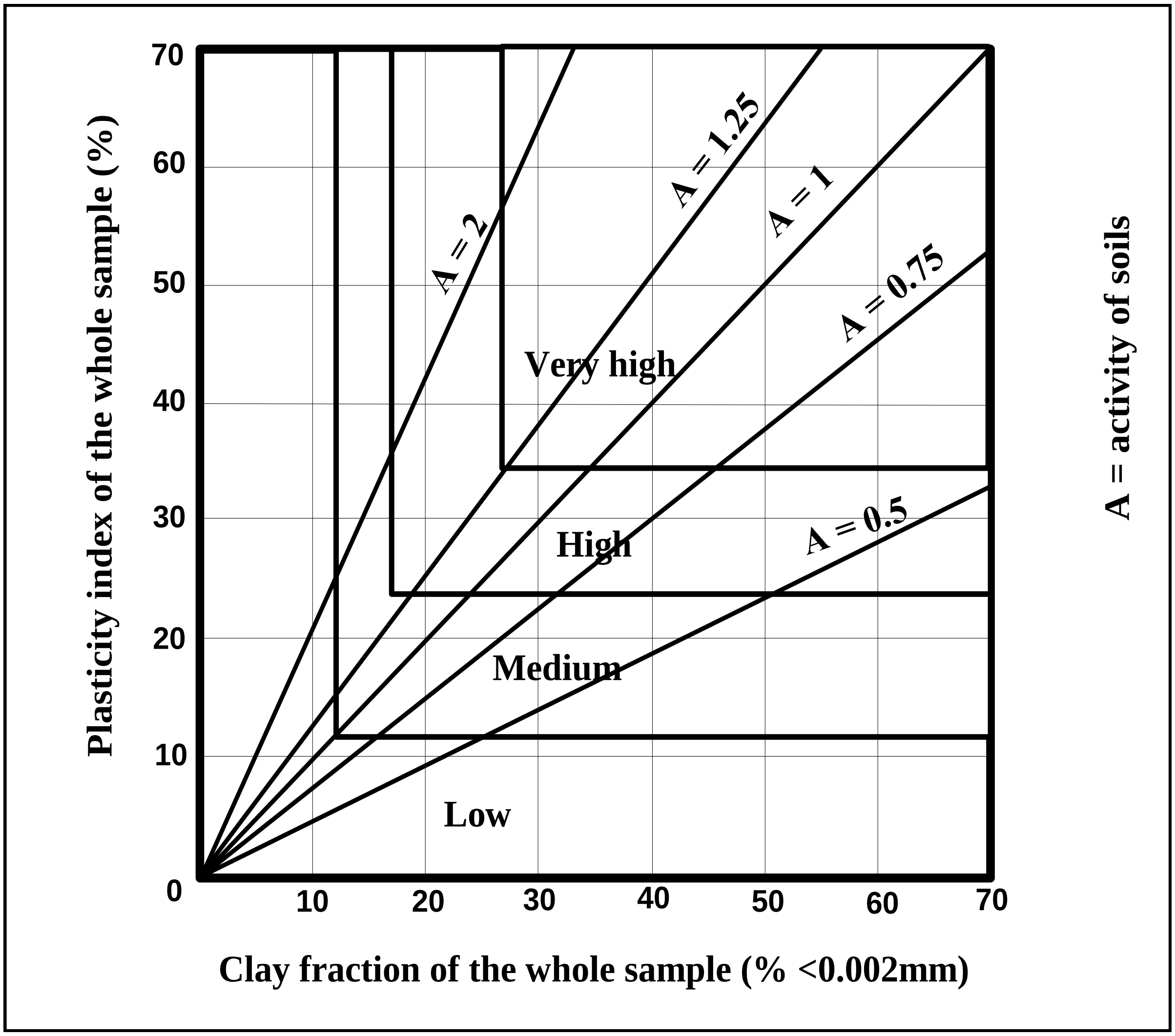

Figure 3.4 Chart for evaluation of potential expansiveness (Seed et al., 1960).

Direct methods provide actual physical measurements of swelling. Several laboratory methods have been developed to directly determine the soil swelling as moisture content changes. These include; free swell and California Bearing Ratio (CBR). One of the more simple procedures is the free swell test (Holtz and Gibbs, 1956). A small sample (10 cm^3) of dry soil passing the No. 40 sieve is added to a graduated cylinder and filled with water. The free swell is determined by comparing the initial volume with the final volume. Bentonite will swell between 1200 to 2000%. Soils having free swell values greater than 100% are considered potential problems, whereas soils with free swell values below 50% probably do not exhibit appreciable volume changes.

3.3.4.5 Activity of soils

The activity (A) of a soil is the ratio of plasticity index (PI) to percent of clay-sized particles (less than 0.002mm) present. Different types of clays have different specific surface areas which controls how much wetting is required to move a soil from one phase to another such as across the Liquid limit or the Plastic limit. From the activity one can predict the dominant clay type present in a soil sample. Kaolinitic and illitic clays are usually inactive while montmorillonitic clays range from inactive to active. High activity signifies large volume change when wetted and large shrinkage when dried. Soils with high activity are very reactive chemically. Normally, the activity of clay is between 0.75 and 1.25, and in this range clay is called normal, when A is less than 0.75, it is considered inactive, when A is greater than 1.25, it is considered active (Skempton, 1953).

3.3.4.6 Classification of soils

Soils in nature rarely exist separately as gravel, sand, silt, clay or organic matter, but are usually found as mixtures with varying proportions of those components. Grouping of soils on the basis of certain definite principles would help the engineer to rate the performance of a given soil either as a sub-base material for roads and foundations of structures, etc. The Classification or grouping of soils is mainly based on one or two index properties of soil which are described in detail in the above sections. The methods that are used for classifying soils are based on grain size distribution and limits of soil. Many systems are in uses that are based on grain size distribution and limits of soil. The systems that are quite popular amongst engineers are the AASHTO Soil Classification System, the Unified Soil Classification System and the system of classification proposed by International Association of Engineering Geology (IAEG). The Unified Soil Classification System (USCS) and International Association of Engineering Geology (IAEG) are the important methods to classification soils for geotechnical investigation of foundations while AASHTO soil classification system is used to classify soils in the case of highway (Murthy, 2002).

3.3.5 Engineering Properties of Rocks

Rocks are involved in most of the civil engineering projects. The rocks may be involved as a foundation material, in excavations or as a slope forming material. The performance of rock as foundation material or to form a stable slope entirely depends upon the properties of the rocks. Rock properties form an important part of the exploration, design and construction of an engineering project. When rocks are loaded by civil engineering structures, these are subjected to displacement. If these rocks are overloaded they may damage by breaking or cracking. The effect of load on rocks depends on the engineering properties of these materials. For engineering purpose rocks may be divided as intact rock and rock mass (Raghuvanshi, 2010).

Intact rock is the term applied to rock containing no discontinuities such as joints and bedding. Sometimes it is also known as "rock material". A rock mass is a mass of rock containing discontinuity planes. For the foundation study, properties of rock mass are important rather than properties of intact rocks. Because the properties of rock mass are reflected the general conditions of the rocks where as intact rock describes the strength of a given materials.

3.3.5.1 Rock Quality Designation (RQD)

The Rock Quality Designation (RQD) was devised by Deere et al. (1967) to provide quantitative estimate of rock mass quality from drill core logs as shown in Table 3.3. RQD is defined as the percentage of intact core pieces longer than 10 cm (4inches) in the total length of core. It is important parameter to describe the engineering properties of rock mass. RQD is determined using the formula described below.

$$RQD = \frac{\sum Length\ of\ core\ pieces}{Total\ length\ of\ core\ run} \tag{3.26}$$

Table 3.3 Standard description of RQD.

Rock Quality Designation (RQD)	Description of Rock Quality
0-25	Very poor
25-50	Poor
50-75	Fair
75-90	Good
90-100	Excellent

CHAPTER FOUR

DATA ACQUISITION, PROCESSING AND PRESENTATION

4.1 Electrical Resistivity of 2D Imaging

4.1.1 Instrumentation and Data Acquisition

The electrical resistivity data was collected using the IRIS instruments SYSCAL R1 plus Switch 72 resistivity meter that utilizes 72 electrodes, through interconnectable four reel cables accommodating 18 electrodes each, 72 short connector wires and two reversible connector boxes (Figure 4.1). The cables used in the particular instrumentation have pick up/connection points spaced at 5m. The instrument records automatically with a present format uploaded into the unit and the system takes measurements almost independently once the array are laid along the profile by selecting four relevant electrodes according to the array type.

Figure 4.1 Instrumentation of 2D electrical imaging.

Reel cables are connected each other with connector boxes and each cable outlet is connected to electrode by the connector wires. A twelve volt external battery was used for this survey. In the survey, the instrument is normally put at the centre, where the deepest depth is recorded, and the four cables reels spread on both side of the resistivity meter. The two cables are in one side of the resistivity meter while the other two are spread on the other side of the resistivity meter (Figure 4.2).

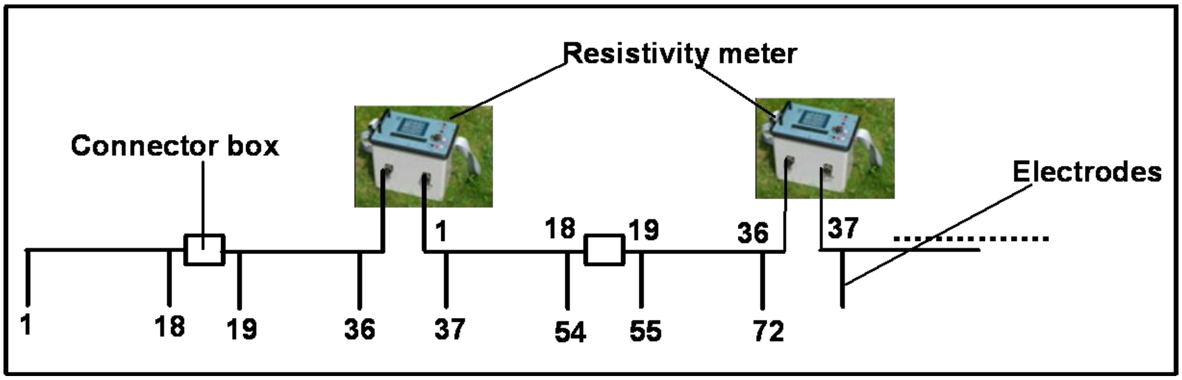

Figure 4.2 General Field layout of 2D electrical imaging, the bottom electrodes for the main sequence where as the top electrodes for the rollalong.

The instrument enables the recording of accurate and reliable measurements through the high power and high sensitivity characteristics. The inter-electrode spacings were reduced to 2 m to attain high spatial resolution data to the reasonably acceptable depth for engineering work to depths of up to 20 - 27 m and were made with the mixed Wenner - Schlumberger array.

A total of four profiles were surveyed and three of these profiles were carried out with horizontal length of 322 m, each profile thus containing one main and five rollalong sequences in order to cover greater length. The orientation of the profiles is almost parallel to each other and inclined from southeast to northwest direction. In addition to these, one profile (a cross profile line) almost at right angles to the three profiles was conducted in order to detect structures potentially oriented parallel to the three profiles (Figure 4.3).

4.1.2 Data Processing and Presentation

The programs installed in the resistivity meter calculate automatically the apparent resistivity from the recorded current, voltage and electrode spacings. These measured data current, voltage and apparent resistivity are stored in the instrument memory. The data downloaded to a computer using the Prosys-II software. The data obtained in the prosys-II software is displayed in tabular form including the electrode distances, apparent resistivity, measured voltage and current, the SP just at the beginning of the resistivity measurement and standard deviation of the reading.

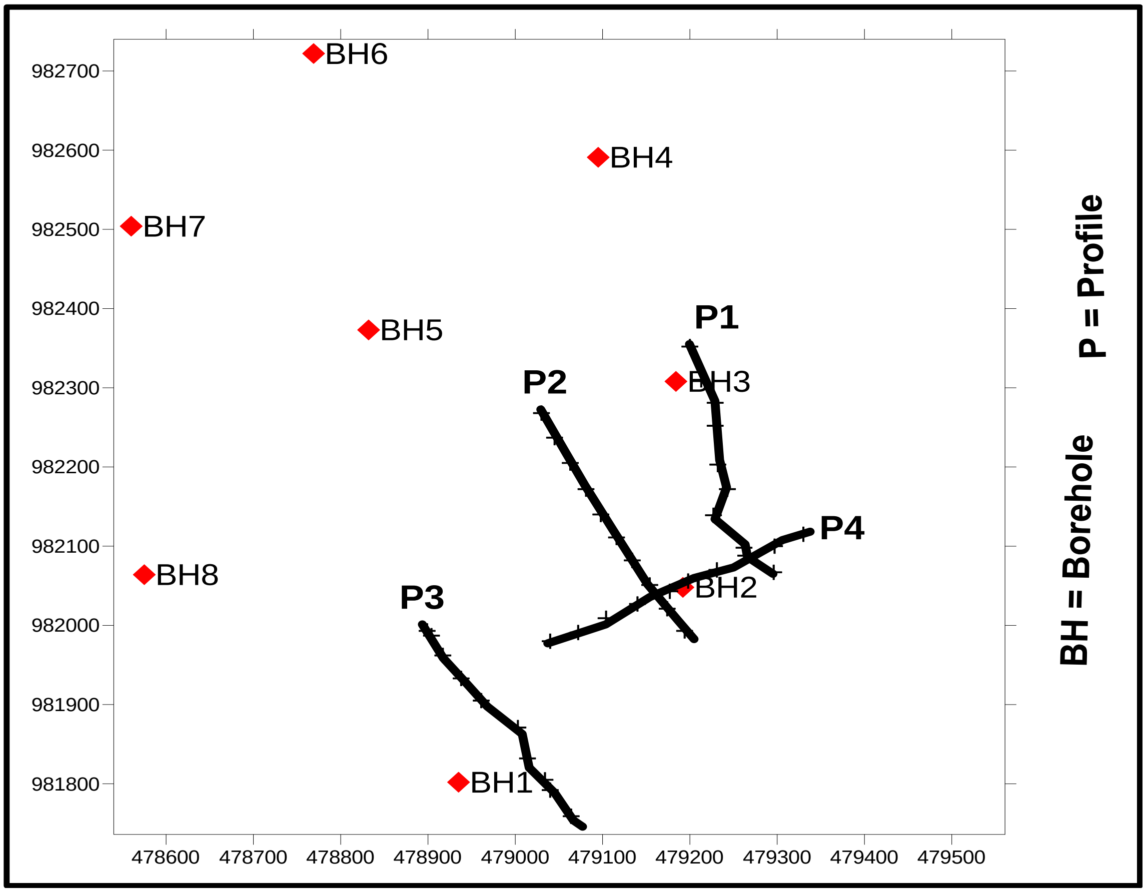

Figure 4.3 Base map of the study area that shows location of electrical 2D survey lines and boreholes

The data obtained in the prosys–II software is started from 90m for each rollalong. Because of this, the rollalong sequences were adjusted with proper distance before add to the main sequence. In the case of rollalong one the data started from 90m, so no distance adjustment is needed. The second rollalong sequence data sheet was recorded after 90 meter of the first rollalong data; it was shifted by 90 meter after getting in the Prosys-II software. This step was continued for the rest rollalong data by increasing total rollalong distance by 90 meter that means 180m to the 3rd rollalong, 270m to the 4th rollalong and 360m to the 5th rollalong. After adjusting the distance, the rollalong sequences were added to the main sequence. Topography is not incorporated to the 2D electrical resistivity section because the project site is on flat terrain.

Even though the electrode spacing arrange with two meter in the ground, the data in the prosys–II software is 5m of electrode spacing. Modification of electrode spacing was done using prosys–II software. The data is filtered using the automating filtering, and exported and saved in RES2DINV.dat format. The electrical resistivity data were processed and inverted using RES2DINV software (Geotomo Software, 2006). For the data obtained in this work, each resistivity cross-section was processed independently. Figure 4.4 shows, for example, the resistivity cross-sections prepared for Profiles-2 using the RES2DINV software. Good quality of data's was used with RMS error of less than 8.2%. Finally the results obtained from the RES2DINV were correlated with the borehole data and magnetic profiles using the surfer 9 software.

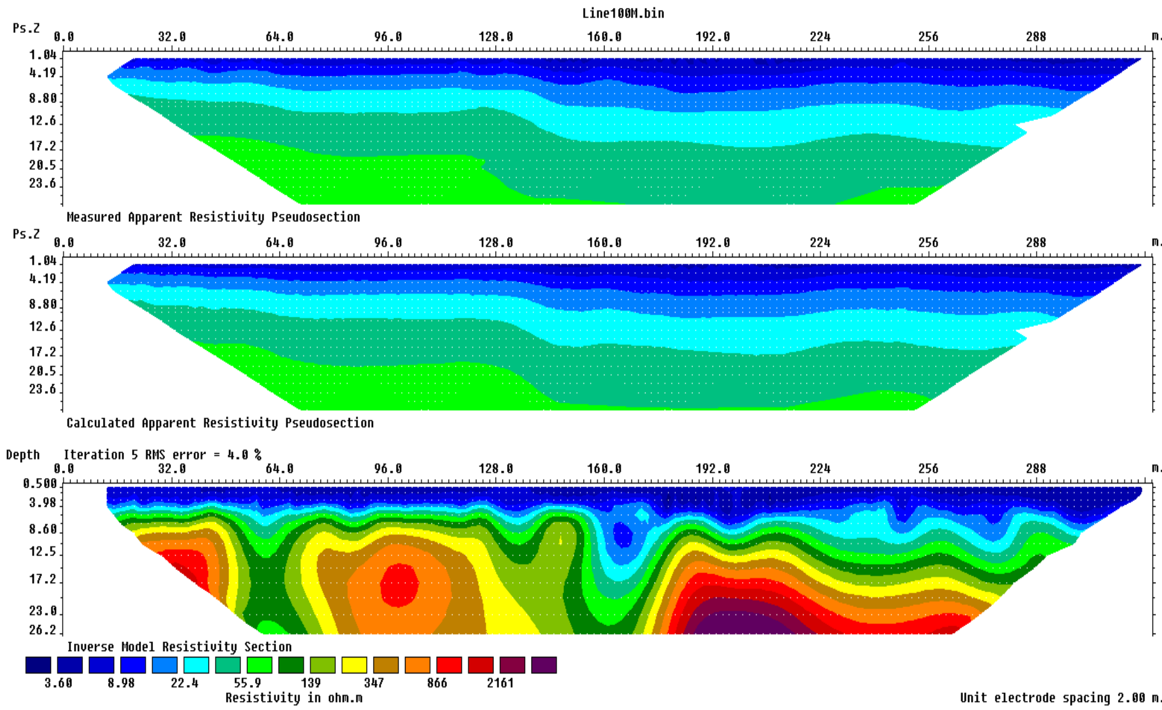

Figure 4.4 Measured and calculated apparent resistivity, and geoelectrical cross-section of Profile-2 resulting from a 2D inversion of data

4.2 Magnetic method

4.2.1 Instrumentation and Data acquisition

Ground magnetic surveys were conducted using the Proton Precision Magnetometer and position location and timings were recorded using the Global Positioning System (GPS) navigational equipment for real-time measurements. The proton precision magnetometer measures the total magnetic field intensity. A base station was carefully selected and established in an area away from the magnetic noise like stores, iron sheet buildings, etc. The location of the base station is within the study area in order to facilitate easy and quick reoccupation. Readings at the base station were taken at every half hour to correct the diurnal variation of the earth magnetic field,

The magnetic data were collected along three profiles and random points. The orientations of the magnetic profiles are similar to the 2D electrical imaging profiles, but the length of the magnetic profiles is much longer. The station spacing used is 10m for all profiles. The random points were collected with station spacing of 30m. The total magnetic data collected during the field survey was 386 data points while 376 data were used for the interpretation (Figure 4.5).

4.2.2 Magnetic Data processing and presentation

The diurnal variation was removed from the observed magnetic field data using the Microsoft excel 2007. The main magnetic field at the base station is obtained from the International Geomagnetic Reference Field (IGRF). The IGRF value at the base station is subtracted from the diurnal corrected total magnetic field of each station. The magnetic field anomaly map was gridded and contoured using the Geosoft software.

Magnetic profile data were picked up from the magnetic anomaly map corresponding to the profiles of the 2D electrical resistivity imaging lines. This helps to counter check and integrating the results from the two methods for detail interpretations.

The total study area with the magnetic survey is of about 1.1 km by 1.1 km dimension and is found within the low latitude magnetic equator. Because the survey covers very small area, the variation of magnetic field with latitude and longitude is insignificant and hence normal corrections were not done. In addition to this, in magnetic equatorial regions where inclination is less than 15 degrees, reduction to the pole is generally unstable and cannot be derived (Getech, 2007). Due to this reason reduction to the pole was not also done.

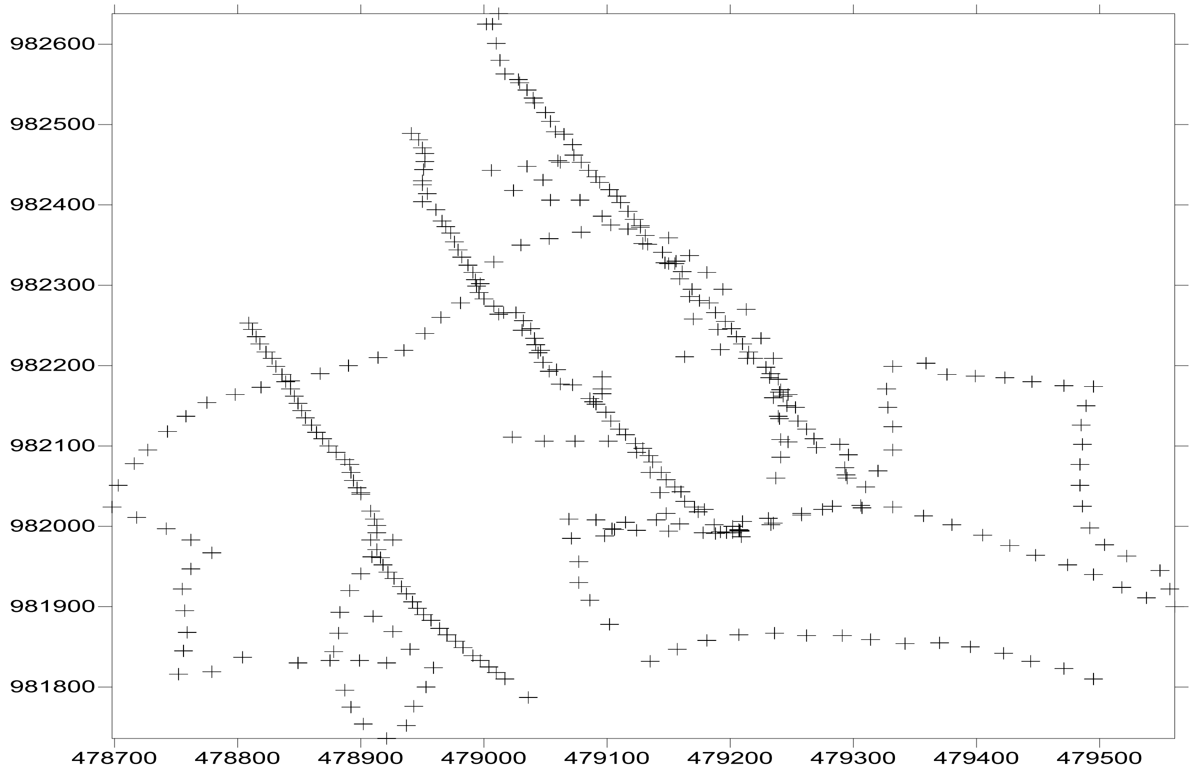

Figure 4.5 Magnetic data distribution.

Rather than reduction to the pole and normal corrections, other data enhancement technique was applied to produce magnetic map, which may helps to highlight particular characteristics or features to aid qualitative interpretation. Analytic signal was done by using Geosoft software package program called MAGMAP.

CHAPTER FIVE

RESULT, DISCUSSION AND INTERPRETATION

5.1 Electrical resistivity 2D imaging and magnetic profiles

5.1.1 Introduction

Meaningful geological interpretations for all profiles were done by integrating the geological information from the boreholes, range of resistivity values from the 2D electrical imaging sections and the magnetic profiles. The borehole data helps to understand the vertical geological section of the study area and to correlate these different units with the electrical sections. The depth of the boreholes used for lithological correlation is 10m; whereas the depths of the electrical tomography sections are about 26 m, i.e. the depth of the geotechnical boreholes is relatively smaller as compared to the depth of the electrical sections. Because of this depth difference, the correlations were done up to the depth of the boreholes, which have necessitated the use of different scales during the correlation. The soil types in the boreholes are clearly distinguished, but in the case of the electrical imaging sections it is difficult to distinguish the soil types, since obviously the different soil types in the borehole are combined in to a layer in the electrical imaging. In the following sections the results of the individual profile lines and their interpretations are presented.

5.1.1.1 Profile-1

After filtering and removing of the noisy data from the 2D electrical resistivity data, 2051 data points were used for the inversion for this profile. By adding the main sequence with five rollalong sequences, the total length of the profile extended to 322m, and its inversion result is given in the Figure 5.1b. The program produced a good inverse model after five iterations showing a good raw data quality. In the overall inversion, the RMS error is 3.4% and was achieved after these iterations. The geoelectrical segments in the inverse model resistivity section of Profile-1 are grouped into three geological layers in conformity with the geological information from the borehole BH-3 in Figure 5.1.

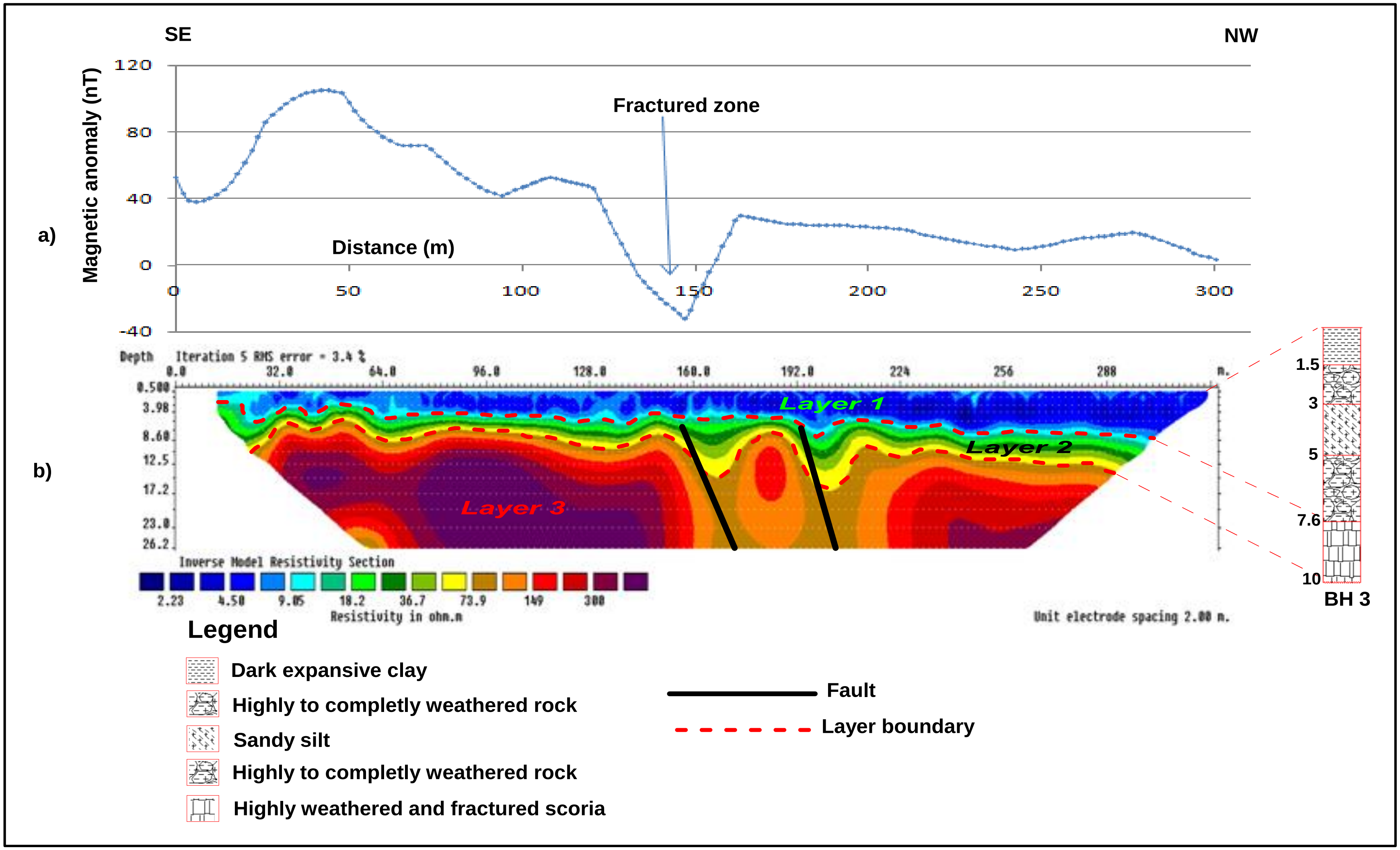

Figure 5.1 Interpretation of profile-1 a) magnetic profile, b) 2D electrical resistivity section.

The resistivity value of the top layer is very low and varies from 2.2 to 9.05 Ω m. These resistivity ranges are the response of recent sediment deposits, which is composed of expansive dark clay, sandy silt and highly to completely weathered rocks possibly containing moisture. The thickness of the layer increases from the southeast to northwest direction and ranges from 3 to 8 m.

The second layer with resistivity ranges of 9.05 – 73.9 Ω m is likely to be the response of the highly to completely weathered and fractured scoria. The thickness of this layer varies from 3 to 8 m with the greater thickness at a distance of 166 m and 198 m from the southeastern side of the line. Due to the presence of weak zones, the materials in those zones are easily weathered and disintegrated into fragments of rocks. The morphology of the layer is undulating and displaced to a depth in the areas where weak zones are found.

The third layer with resistivity greater than 79.3 Ω m is the response of the bedrock. Its resistivity varies considerably along the profile. There are very low resistivity values along the profile, particularly in the area where the weak zones are depicted. This low resistivity in some of the areas within the profile line is possibly due to intensive degree of weathering and water percolation from the surface along the fractures.

Depth to the bedrock ranges from 8.6 to12.5 m and it is shallower in the southeastern side of the line as compared with the northwestern side of the 2D electrical section. The bedrock is seen to have been broken in to three blocks. The one block on the northwestern side appear to have relativly moved downward compared to the blocks in the southeastern side. From these electrical signatures, the two fractures could be interpreted as normal faults.

The magnetic profile along the 2D electrical imaging of Profile-1 was plotted as shown in the Figure 5.1a. This profile shows considerable amplitude variation in the magnetic anomaly signatures. The minimum negative peak value is -32.2 nT at a distance of about 147 m and the maximum positive peak value is 104.9 nT at a distance of about 44 m from the southeastern end of the line. There is indeed a positive correlation between the magnetic anomaly plot and the 2D electrical profile in detecting the weak zones. The magnetic anomaly plot shows a presence of fractured zone at the center of the profile which are also interpreted as faults from the 2D electrical imaging plot. The magnetic anomalies on the southeastern side is high as compare to northwestern side, possibly this indicating a depth increase to the top of the bedrock in the northwestern part.

5.1.1.2 Profile-2

After filtering out the noisy data from the 2D electrical resistivity raw data, a total of 2040 data points were used for the inversion. Integrating both the main sequence and five rollalong sequences, the length of the profile is 322m, produces the inversion section plot shown in Figure 5.2b. The program has applied inverse model by iterating just five times to yield a quality data with RMS error of 4.8 %. This profile could be classified into three different layers in correspondence with the geological information from borehole BH-2 in Figure 5.2.

The first layer shows a very low resistivity anomaly that varies from 3.68 to 22.4 Ω m. This layer is similar to the first layer in Profile-1 which is a recent sediment deposit, which is composed of expansive dark clay, silty clay/clayey silt and sandy silt. Like the first layer in Profile-1, the thickness of the layer increases from southeast to northwest direction. This varies from 5 to 12.5 m and has maximum thickness nearly at the center of the line which is 166m from the southeastern point of the profile. The greater thickness of soil at this zone could be due to the high degree of weathering along the fractures.

The resistivity of the second layer ranges from 22.4 to 347 Ω m which is possibly the response of highly to completely weathered scoracious basalt. Analogous to the first layer, its thickness is increasing from southeast to the northwest direction. Thickness of this layer varies from 4 to 10 m on both sides of the section, but its thickness is greater than 26m at the zones extending from 48 to 76 m and 128 to 180 m distance from the southeastern side of the profile. The thickness at those zones become greater in comparison to other zones due to the presence of weak zones which are attributed to the intensively weathered and fractured Earth materials resulting a fragments of rocks. Similarly, to the second layer in the profile-1, the morphology of the layer is undulating and displaced to a depth in the areas where weak zones exists.

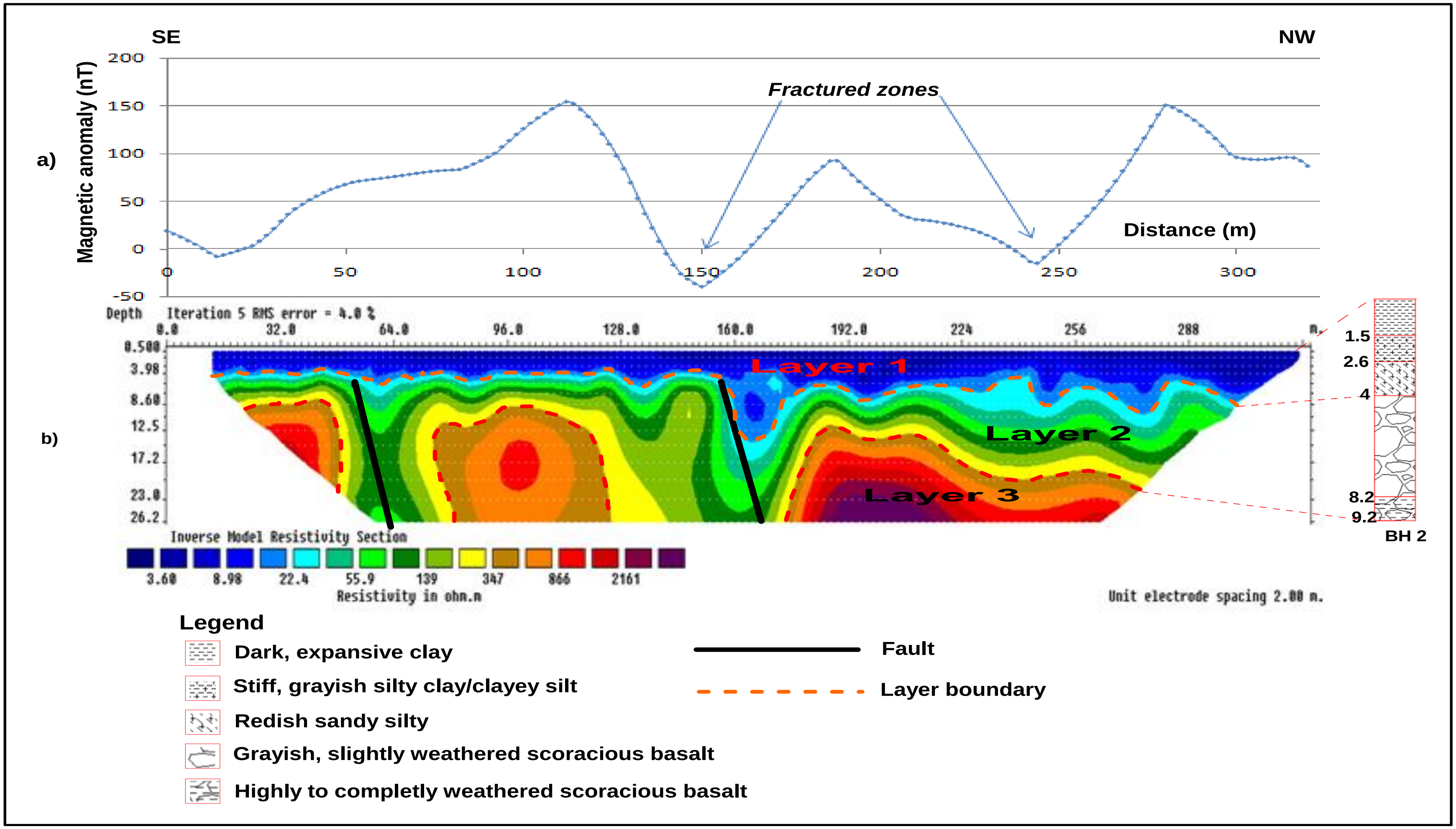

Figure 5.2 Interpretation of profile-2 a) magnetic profile, b) 2D electrical resistivity section.

The third layer with resistivity greater than 347 Ω m is the response of fresh to slightly weathered scoracious basalt. It is a bedrock in the local area and is characterized by the increment of depth from southeast to northwest direction, with depths of 10 m in the southeastern and 20 m on the northwestern of the 2D electrical resistivity section as shown in Figure 5.2b. The morphology of the bedrock is again undulating. Equivalent to the bedrock mapped in Profile-1, it is broken in to three blocks. The two blocks on the northweatern side are moved downward compared to the block on the southeastern side of the section. Therefore, the weak and fractured zones may possibly interpreted as normal faults. The location of these faults are at a distance of 48 and 154m from the southeastern side of the profile.

The magnetic profile along the 2D electrical imaging line, Profile-2, is also plotted as shown in the top section of the 2D image in Figure 5.2a. The extreme values, the minimum negative peak value of -39 nT at a distance of about 150m and the maximum positive peak value of 154 nT at a distance of about 120m from the southeastern point. The magnetic field profile almost coincides with the 2D electrical resistivity profile in identifying the weak zones. Very close to the middle of magnetic profile, the plot shows the presence of fractured zone which might be interpreted as normal fault from the 2D electrical imaging plot. In addition to this, there is also an indication of a fractured zone at the distance of about 240m from the southeastern end of the survey in the magnetic plot which is not clearly exposed in the 2D electrical resistivity imaging.

5.1.1.3 Profile-3

A total of 2043 filtered 2D electrical resistivity data were used for the inversion model. The length of this profile is again 322m resulting from a combination of a main sequence and five rollalong sequences. The inversion result is shown in Figure 5.3b. The program produced good inverse model after iteration of about five time and showing a good data quality with RMS error of 8.2%. This profile could be again classified into three different layers in agreement with the geological information from borehole BH-1 in Figure 5.3.

The 2D electrical resistivity section obtained on this line is characterized by a high degree of fracturing. Along the profile, the resistivity value of the top layer is very low and varies from

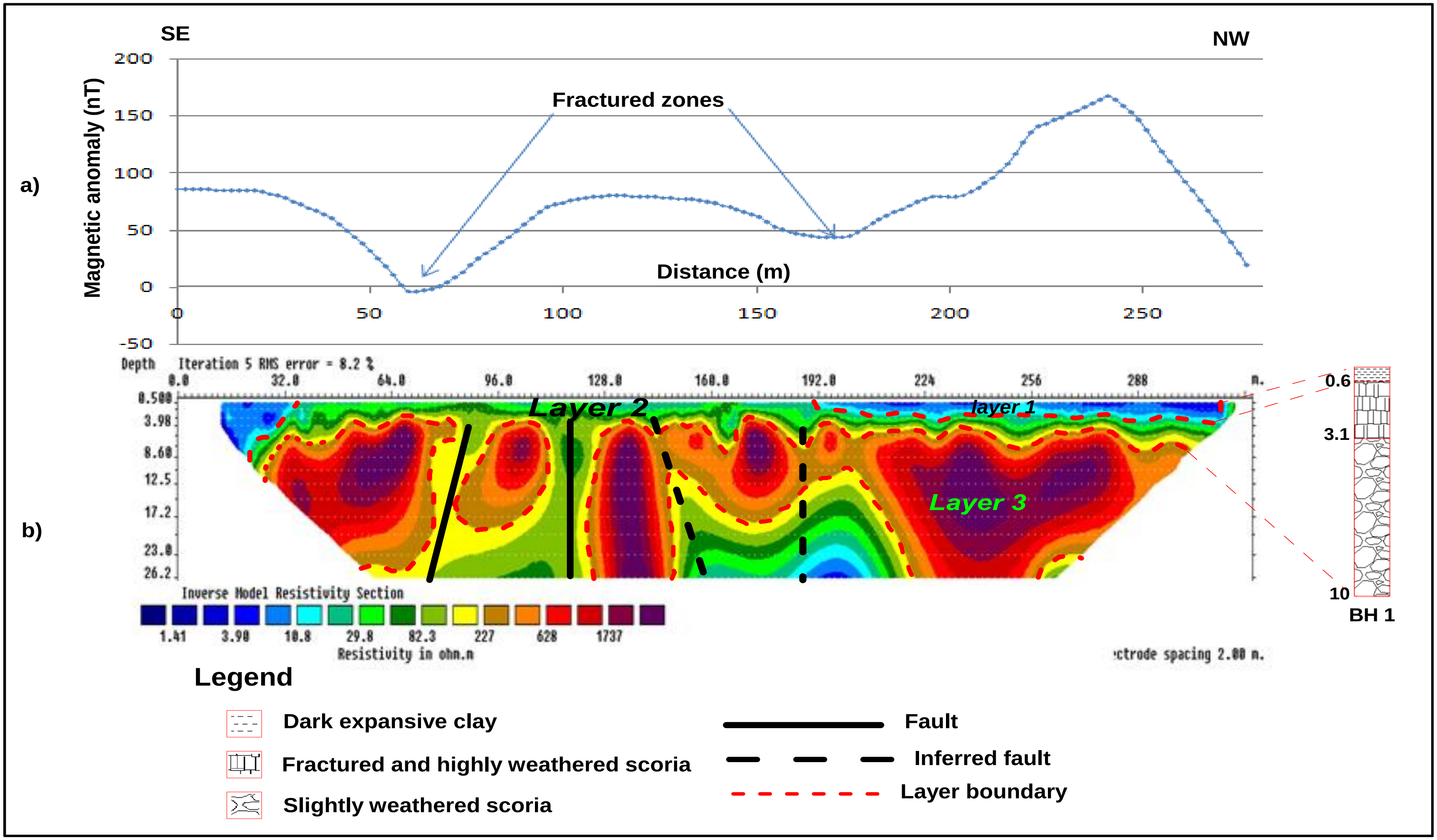

Figure 5.3 Interpretation of profile-3 a) magnetic profile, b) 2D electrical resistivity section.

1.41 to 10.3 Ω m and these resistivity respsones are that of the dark expansive clay. As compared with the first layer in the other three profiles, this layer is relativly thinner and discontnious. It is found on both sides of the 2D electrical resistivity section and is almost absent at the zones from 36 to 194 m distance from the southeastern point of the line. The thickness of the layer ranges from 3.1 to 8 m.

The second layer with resistivity range of 29.8 – 227 Ω m is the response of the slightly to highly weathered and fractured scoria. Generally, the thickness of this layer varies from 3 to 4 m. Similar to the second layer in Profile-2; its thickness is greater than 26.2m along the profile particularly in the area where weak zone is present.

The third layer is found at a depth ranging from 4 to 8 m with a highly fractured and weathered zone that shows a significant resistivity variation within it. When one sees the four profiles side by side, the depth to the bedrock is relatively the shallowest on this profile. The bedrock appears to be a single unified block which was later broken apart into a number of blocks due to the tectonic actvities. There are four fractures that could be interpreted as faults on this line.

There is also very low resistivity zone at the bottom of the third layer similar to the second and first layers. This zone is found within the depth of (23 – 26.2 m) at the distance between 144 - 208 m from the preliminary southeasten side of the profile. It is bounded by two fractures which are interpreted as faults. The depth of water table in the area, which appears to be the shallowest on this profile, is 24m. Therefore, the very low resistivity at the greater depth is possibly due to high degree of weathering and water percolation from the surface along the fractures.

Magnetic profile along the same line on which the 2D electrical imaging of Profile-3 was plotted as shown on the top of 2D electrical resistivity imaging Figure 5.3a. The minimum negative peak value is -4 nT at a distance of about 60m and the maximum positive peak value is 168 nT at a distance of about 240m from the initial station position on the southeastern side of the line. The magnetic field profile roughly coincides with the 2D electrical resistivity profile plot to identify the weak zones. The magnetic profile clearly shows the presence of two fractured zones which could also be interpreted as faults from the 2D electrical resistivity section.

5.1.1.4 Profile-4

Contrary to the above three survey lines, this survey traverse runs almost perpendicular to them and is oriented roughly from the northeast to southwest direction. In so doing, the line cuts the traverse lines 1 and 2. It is intended to map possible structures that may be oriented almost parallel to the three profiles as discussed above.

Following a careful unwanted data elimination and filtering process of the 2D electrical resistivity raw data, a toatl of 2011 data points were used for the inversion modeling on this profile. The length of the Profile extends to 322m. The model has been represented from a combination of a main and five rollalong sequences. The inverted 2D electrical resistivity section for the profile is as shown in Figure 5.4b. The program produced a good quality inversion model again after five iterations resulting in acceptable RMS error of 4.4%. In correlating the section with the available borehole close by BH-2, the same number of layer like in the other profiles discussed above were obtained although the line was unique in that it is surveyed orthogonal to the rest of profiles. This shows there is not much directional property/anisotropy in the subsurface layers.

The first layer of the segment signaled a very low resistivity ranging from 3.02 to 15.2 Ω m analogous to the responses from the other profiles for the first layer. This layer is the result of a recent sediment deposit that is composed of expansive dark clay, silty clay/clayey silt and sandy silt. The thickness of the layer varies from 4 to 10 m.

The second layer with resistivity range of 15.2 – 172 Ω m is possibly the response of slightly to highly weathered scoracious basalt. The thickness of this layer varies from 4 to 6 m on both sides of the section. The greater thickness of the layer is found at the distance of 104 m and 184 m from the starting point (northeastern side of the line) in the weak zones with easily weathered and disintegrated materials. Like the second layer in the Profiles-1 and 2, the morphology of this layer is undulating and extends to larger depth in the areas where the weak zones exists.

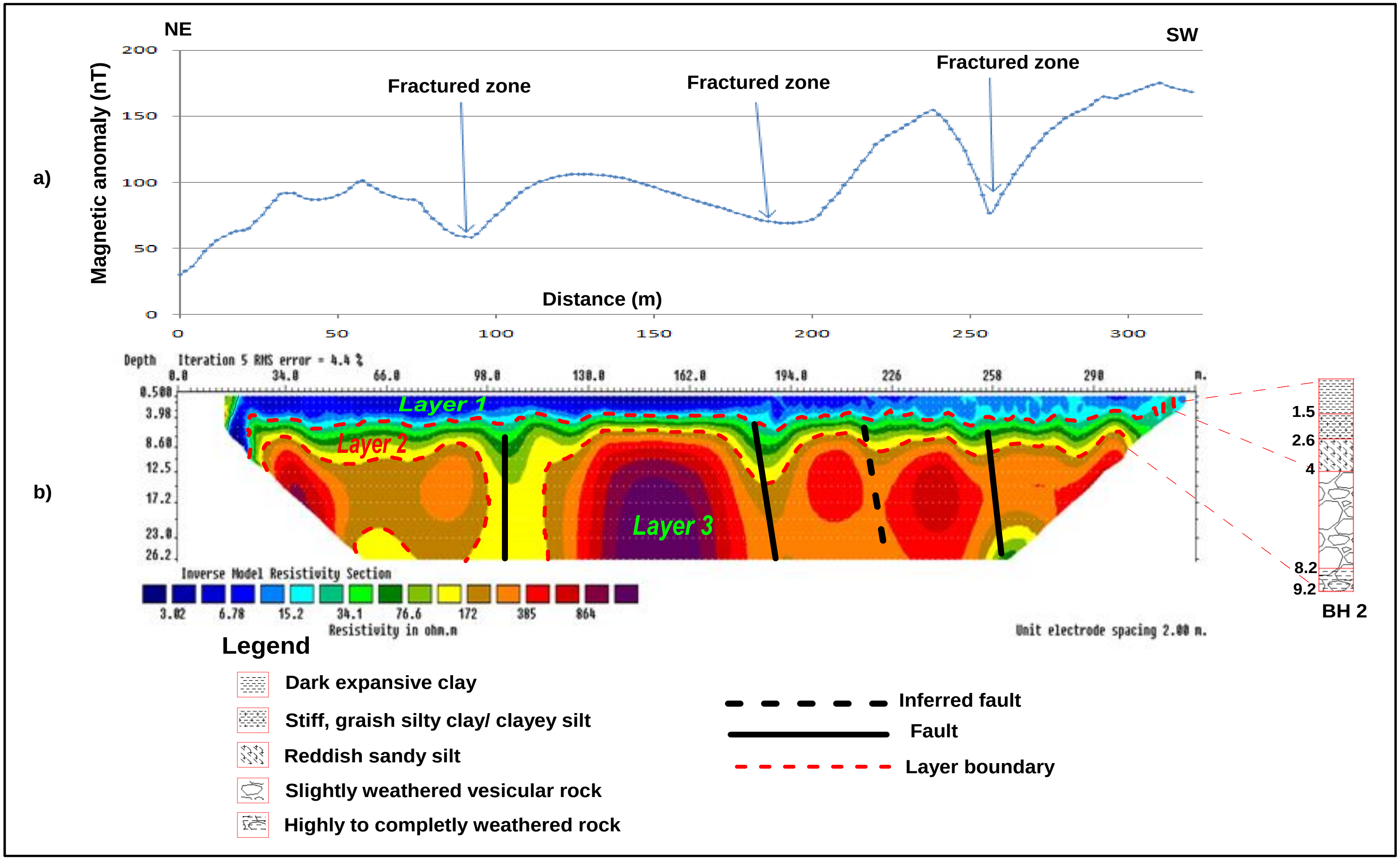

Figure 5.4 Interpretation of profile-4 a) magnetic profile, b) 2D electrical resistivity section.

The third layer with resistivity greater than172 Ω m is the the response of the bedrock. A rough bedrock layer is mapped at depth varies from 8 to 14.85m. It is a highly fractured layer due to various tectonic activities that might have occurred over the area, owing to its location visa-vis the western margin of the rift. Four fracture zones with vertical to near vrtical orenietation are mapped on the profile.

The magnetic profile along the same 2D electrical imaging of Profile-4 was plotted as shown on the top part of Figure 5.4, in Figure 5.4a. This profile shows considerable varying amplitude of magnetic anomaly signatures. The minimum negative peak value is -25 nT at the starting point and maximum positive peak value is 175 nT at a distance of about 314m from northeastern side of the profile. The magnetic profile is more or less overlapped with the 2D electrical resistivity profile in mapping the weak and fractured zones. The magnetic profile shows an indication for the presence of three fractured zones which could be also interpreted as faults from 2D electrical resistivity section.

5.1.2 Combination of the 2D electrical resistivity profiles

Figure 5.5 illustrates how the three 2D electrical resistivity sections of Profile-1, Profile-2 and Profile-3 can be arranged horizontally to give a volume representation of the area. This way of representation is important to understand the continuity of the weak zones within the survey area. The plot clearly depicts that there is continuous fractured zone within the three profiles denoted by letter A (Figure 5.5). There are also localized fractured zones in the profile-2 and 3 symbolized by letter B. From this the building will be preferably constructed in the northwestern side of the profile-1and 3, and southeastern side of the Profile-1 where there are few weak zones and relatively shallow depth to the bedrock.

5.2 Apparent resistivity sliced depth map

Understanding on vertical and lateral distribution of electrical resistivity at the subsurface gives a complete geological framework of the survey area. When the sliced depth sections are at hand in stacked plot form, it provides a simple visualization of the overall picture of the subsurface Earth materials.

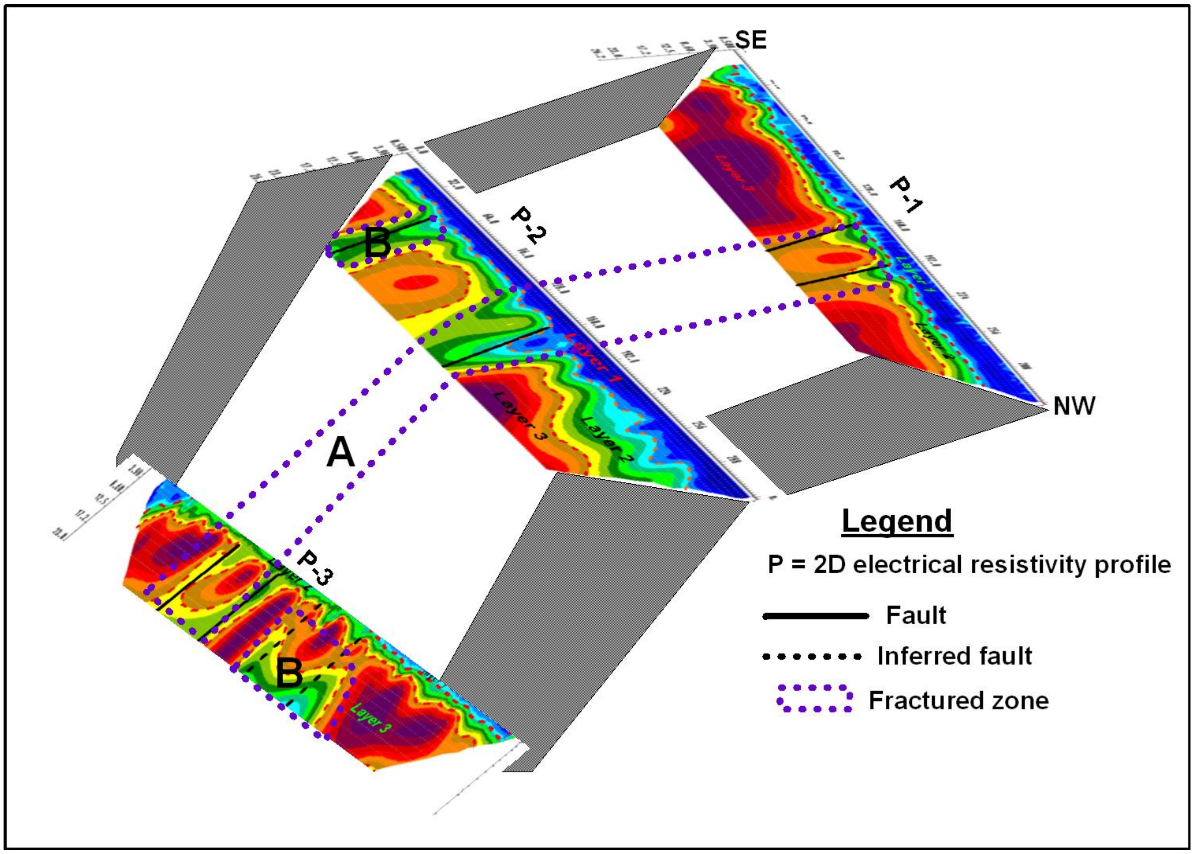

Figure 5.5 Diagram showing how Profile-1, Profile-2 and Profile-3 can be horizontally stacked to give a volume representation.

The apparent resistivity sliced depth map was prepared from the 2D electrical resistivity values at five different depths (Figure 5.6). The map plot shows lateral and vertical variation of relative apparent resistivity of the whole area at the selected depths. The apparent resistivity value varies from 0 to 180 Ohm-m. Based on the resistivity value, the sliced map could be classified in to three zones.

Zone-I is characterized by relatively very low resistivity which ranges from 0 to 30 Ohm-m. This low resistivity is likely the response of recent sediment deposits. Most of the survey area at the depth of 2.624m is covered by recent sediments except the southwestern part which is possibly the response of weathered, fractured scoria and scoracious basalt (Figure 5.6). The surface area coverage of this zone is decrease with depth and absent at the depth of 20.44m. This implies that the thickness of sediments is less than 20 m.

Zone-II is distinguished by relatively intermediate resistivity values ranging from 30 to 110 Ohm-m. Contradictory to zone-I, the surface area coverage of this zone is increasing with depth. At the depth of 2.624m, it covers the southwestern part of the survey area. The integrated results obtained from the 2D electrical resistivity imaging profiles and borehole data the intermediate resistivity value could be the response of highly to completely weathered and fractured scoria, scoracious basalt and basalt.

Zone-III is characterized by relatively high resistivity as compared with the rest of zones which ranges from 110 to 180 Ohm-m. This zone starts at the depth of 4.186 m which covers a small portion of the study area in the southwestern part. Analogous to zone-II, the surface area coverage is increasing with depth. The result obtained from the 2D electrical resistivity profiles indicates that the high resistivity value could be the response of the bedrock. Based on stacked resistivity pseudo-section map, depth to bedrock is relatively shallow at the southwestern, western, and southern part of the study are, as a result, those parts of the study area are better for building foundations.

5.3 Magnetic anomaly and analytical signal maps

5.3.1 Magnetic anomaly map

The raw magnetic data were corrected for diurnal variation and removal of anomalous instrumental readings through close examination of the data. IGRF determined values were then used to reduce the resulting data to the magnetic anomalies. The final data used to draw the magnetic anomaly map of the study area which shown in Figure 5.7. From the plot, the area was divided into three zones. In the map the zones represented by letter **A** shows high magnetic anomaly relatively to the other regions. The high magnetic anomaly response is probably due to the result of highly magnetized volcanic rocks that could be found in the area. It covers the southwestern, southern, eastern and central part of the study area.

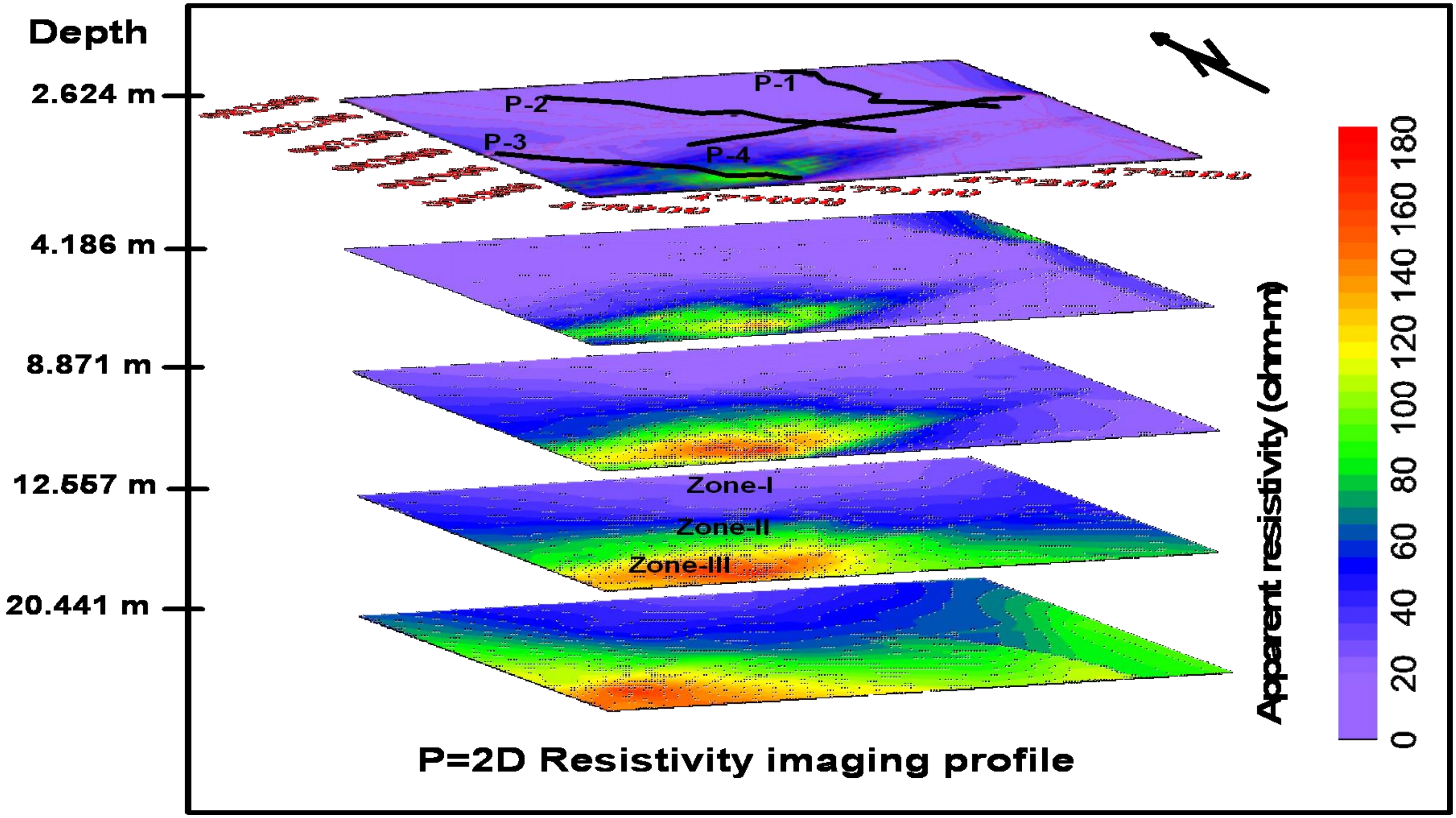

Figure 5.6 Apparent resistivity sliced-stacked depth maps.

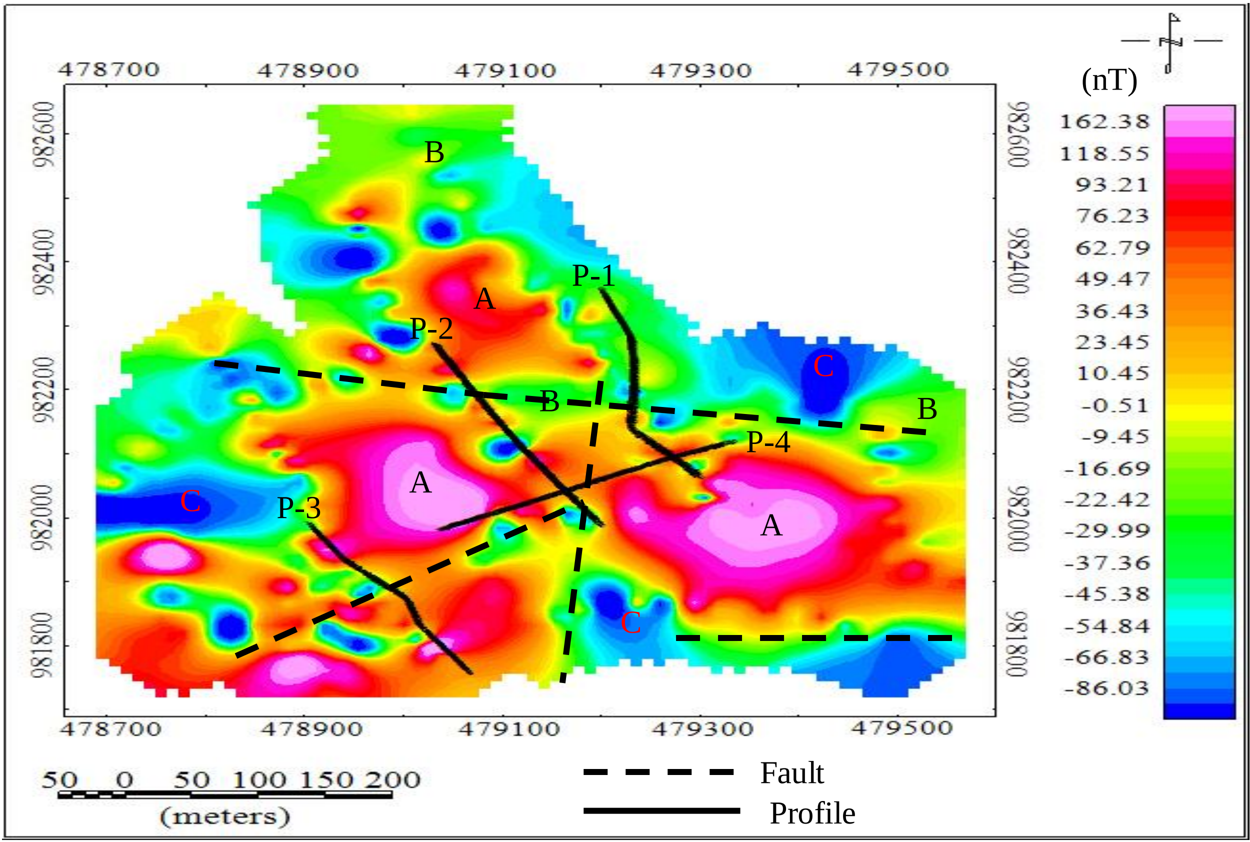

Figure 5.7 Magnetic anomaly map of the study area.

The intermediate and low magnetic anomaly zones are represented in the map by letter **B** and **C** respectively. It covers the northeastern, northwestern and southeastern parts of the survey area. The possible geological structures are plotted in the magnetic anomaly map based on the structures on the magnetic and 2D electrical resistivity profiles and features on the magnetic anomaly map (Figure 5.7).

5.3.2 Analytical signal map

From the magnetic data it was possible to construct an analytical signal map shown in Figure 5.8. The analytic signal has a form over causative bodies that depend on the locations of the bodies but not their directions of magnetization. Furthermore, the map (Figure 5.8) shows the responses of anomalous bodies just from the upper part of their sources. It is seen from the map that there are distinct areas where the relatively competent rock units are widely spread over the area and are found at shallower depths. If the results of this survey were to be employed during the design of the buildings, areas which can support heavy structures and areas that need special design considerations are clearly outlined.

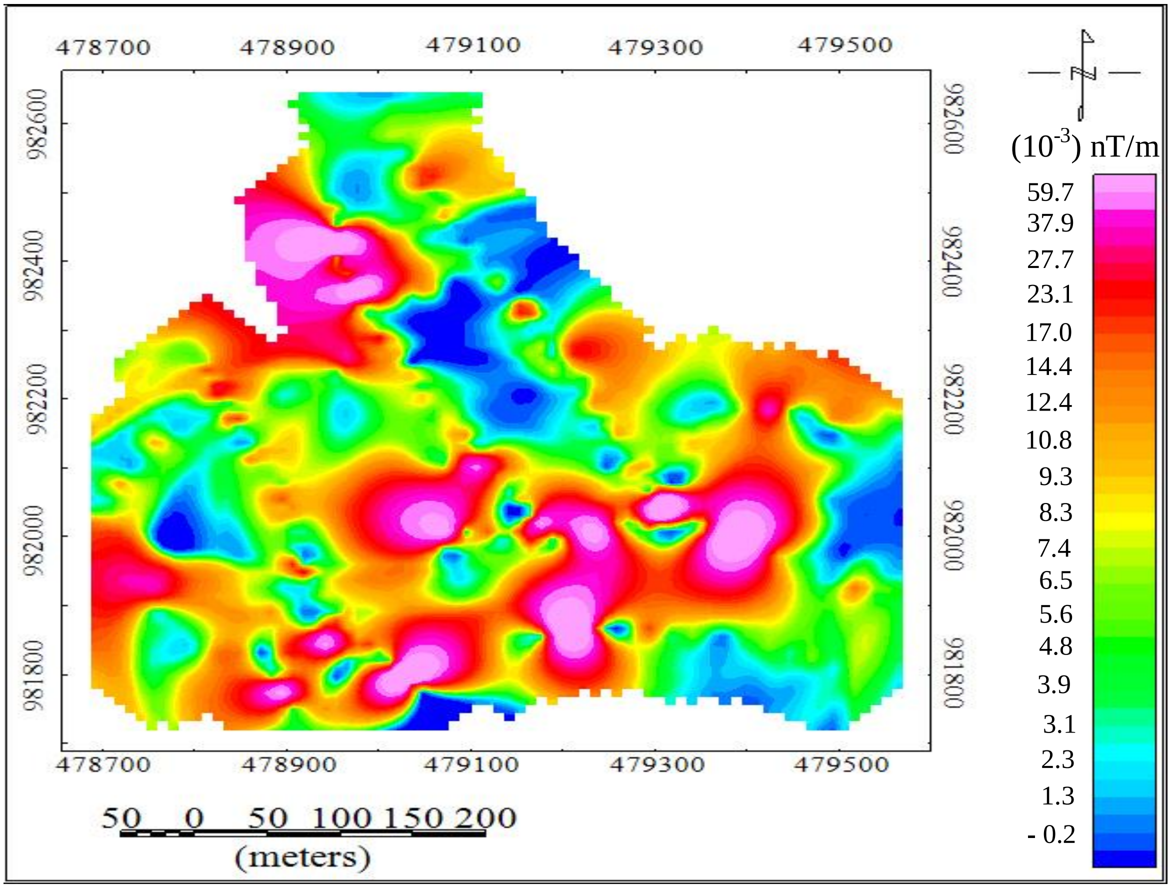

Figure 5.8 Analytical magnetic anomaly map of the study area.

5.4 Engineering properties of soils

5.4.1 Description of Soils

The project site is covered by recent sediment deposits with variable thickness. This is observed in the field from the foundation excavations and depicted in Figures 5.9. From those sections and close examination of the materials, it was observed that the soils are grouped into clay, sandy silt, clay/clayey silt and granular materials. The clay soil is generally black in color, firm to stiff expansive nature and covers the entire part of the site. The silty clay/clayey silt soil is mainly residual in origin and their color is yellowish to dark-grey. It is mostly found underlying the clay soil. The granular materials (Figure 5.9b) are the product of intense weathering, fracturing and disintegration of basaltic and scoracious rocks. Mostly, it is greyish or reddish, very dense mixture of gravels and rock fragments.

Figure 5.9 a) Photo of vertical section of the geology of the project site from the central (a) and southern (b) part of the survey area.

5.4.2 Index properties of soils

5.4.2.1 Natural Moisture Content (NMC) and Specific gravity

Water content can have a significant effect on the soils' behavioral properties when used for construction purposes and foundations. Moisture content affects the settlement (consolidation) condition, shear strength and suitability of soil for compaction. Particularly the consistency of fine grained soil depends largely on its moisture content. From the laboratory results, the natural moisture content and specific gravity of soils of the area are described in tabular form (Table 5.1). The average natural water content of the study-area soils was found to be 30.62 %, with a range extending from 22.31 % to 35.56 %. The specific gravity of the soils is 2.45.

Table 5.1 Natural moisture content and specific gravity of soils of the project site.

Sample No	BH No	Depth (m)	Natural Moisture Content (NMC) (%)	Specific gravity
1	4	3	32.45	2.45
2	4	5	32.27	2.45
3	3	2.5	30.12	2.45
4	3	4.5	22.36	2.45
5	3	6.5	35.56	2.45
6	5	3	32.84	2.45
7	6	3	31.47	2.45
8	6	8.3	27.91	-

5.4.2.2 Grain-size Analysis

The laboratory results of grain-size analysis are presented in Appendix-3. From this result, the grain size distribution curves were plotted in which the grain size as the abscissa on the logarithmic scale and the percent of finer as the ordinate on the arithmetic scale (Figure 5.10).

The shape of the curves indicate the proportion of the soil size particles on the given soil samples. The curves shows missing of certain particle size of soils (Figure 5.10). Therefore, the soils of the study area are grouped as gap graded soils.

The range of grain-size results are given in Table 5.2, which indicates the fine-grained nature of the soils. The grain-size analysis showed that the fine-grained soils are composed of 1.48 - 14.72 % sand, 32.58 - 55.28 % silt and 30 - 64.5 % clay-size particles. The gravel size soil particles are absent in all the soil samples. In the case of fine grain soils water content is a major factor rather than size of the particles, especially when the soil contains active clays. Therefore, it is important to determine the Atterberg limits for better understanding the engineering properties of fine grain soils.

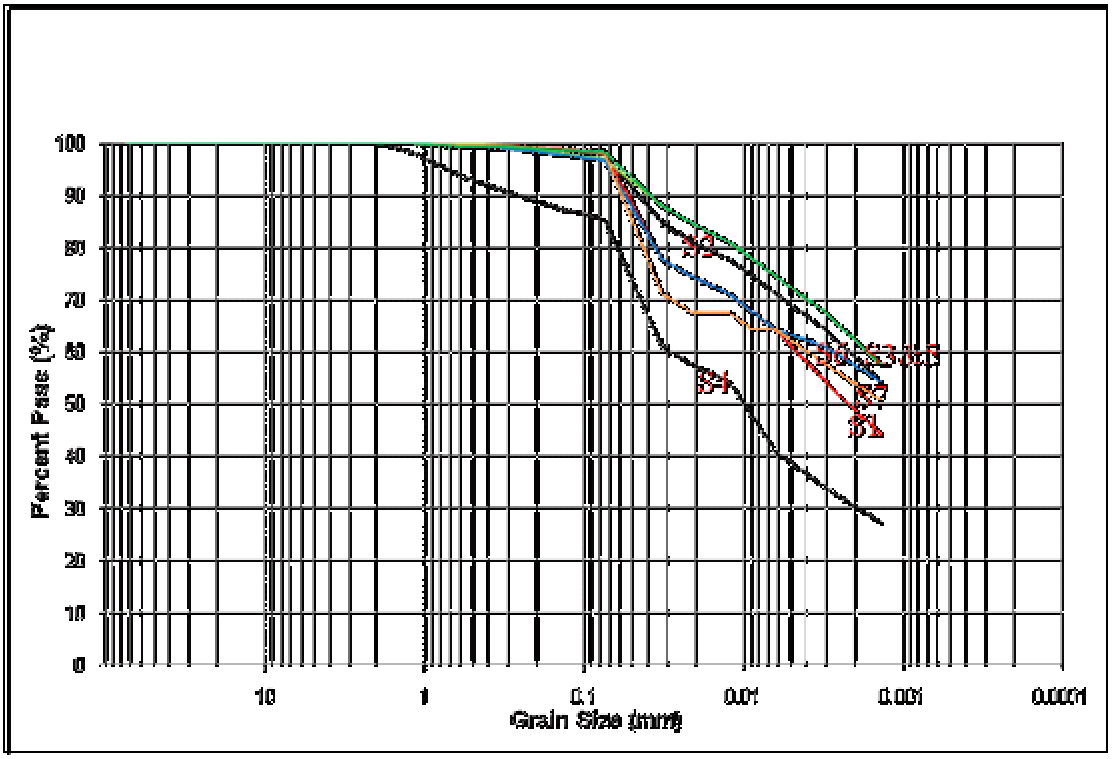

Figure 5.10 Grain-size distribution curves of soils of the project site.

Table 5.2 Grain-size analysis results of the soils of the study area.

Sample No	Borehole No	Depth (m)	Gravel	Sand	Silt	Clay
			%			
S1	1	3	0	1.5	49.5	49
S2	4	5	0	2.1	37.9	60
S3	3	2.5	0	1.48	34.02	64.5
S4	3	4.5	0	14.72	55.28	30
S5	3	6.5	0	2.92	32.58	64.5
S6	5	3	0	3.18	39.32	57.5
S7	6	3	0	1.92	43.58	54.5

5.4.2.3 Atterberg (consistency) limits and Plasticity Index

Plastic index and liquid limit are important in classifying fine-grained soils and is fundamental to the plasticity chart. The larger the liquid limit, the greater will be the engineering problems associated with using the soil as an engineering material, such as foundation support for residential building and road sub grades (Bowles, 1992). The result of Atterberg limits of soils of the area are presented in Table 5.3. The Atterberg limits of soils of the survey area ranges from 52.23 to 96.50 %, 36.77 to 49.52 % and 15.46 to 46.98 % corresponding to Liquid Limit (LL), Plastic Limit (PL) and Plasticity Index (PI) respectively. The comparison of liquid and plastic limits with the natural moisture content helps to know the state of soils during the time of sampling. The natural moisture content values are less than the plastic limit values; consequently, the soils were in the solid or semisolid state during sampling. Because of their natural moisture contents less than their liquid limits, as a result, the soil samples were not show the viscous flow behavior during sampling.

Table 5.3 Atterberg limits, activity and free swell soil of the project site from different depths.

Sample No	BH No	Depth (m)	Atterberg limits			Activity	Free swell %
			LL (%)	PL (%)	PI (%)		
2	4	5	72.80	40.15	32.65	0.5	80
3	3	2.5	79.50	42.12	37.38	0.65	130
4	3	4.5	52.23	36.77	15.46	0.24	90
5	3	6.5	96.50	49.52	46.98	0.86	140
6	5	3	80.25	42.85	37.4	0.62	140
7	6	3	70.75	39.12	31.63	1.1	130
8	4	3	85.75	44.26	41.49	0.85	130

5.4.2.4 Swell potential of soils

The study area has geological and climatic conditions which are favorable for the formation of clay soils. So, it is necessary to study swell potential of soils. The free swell soils of the survey area vary from 90 to 140% as shown in Table 5.3. According to the Arora (1997) soils with free swell less than 50% are not likely to show expansive properties, while soils with free swells greater than 50% should have swell problems. When the value of the free swell is 100% or greater are associated with clay, which could swell considerably, even under light loading. The swell potential of soils of the area based on percentage clay fraction and plasticity index are shown in the Figure 5.11.

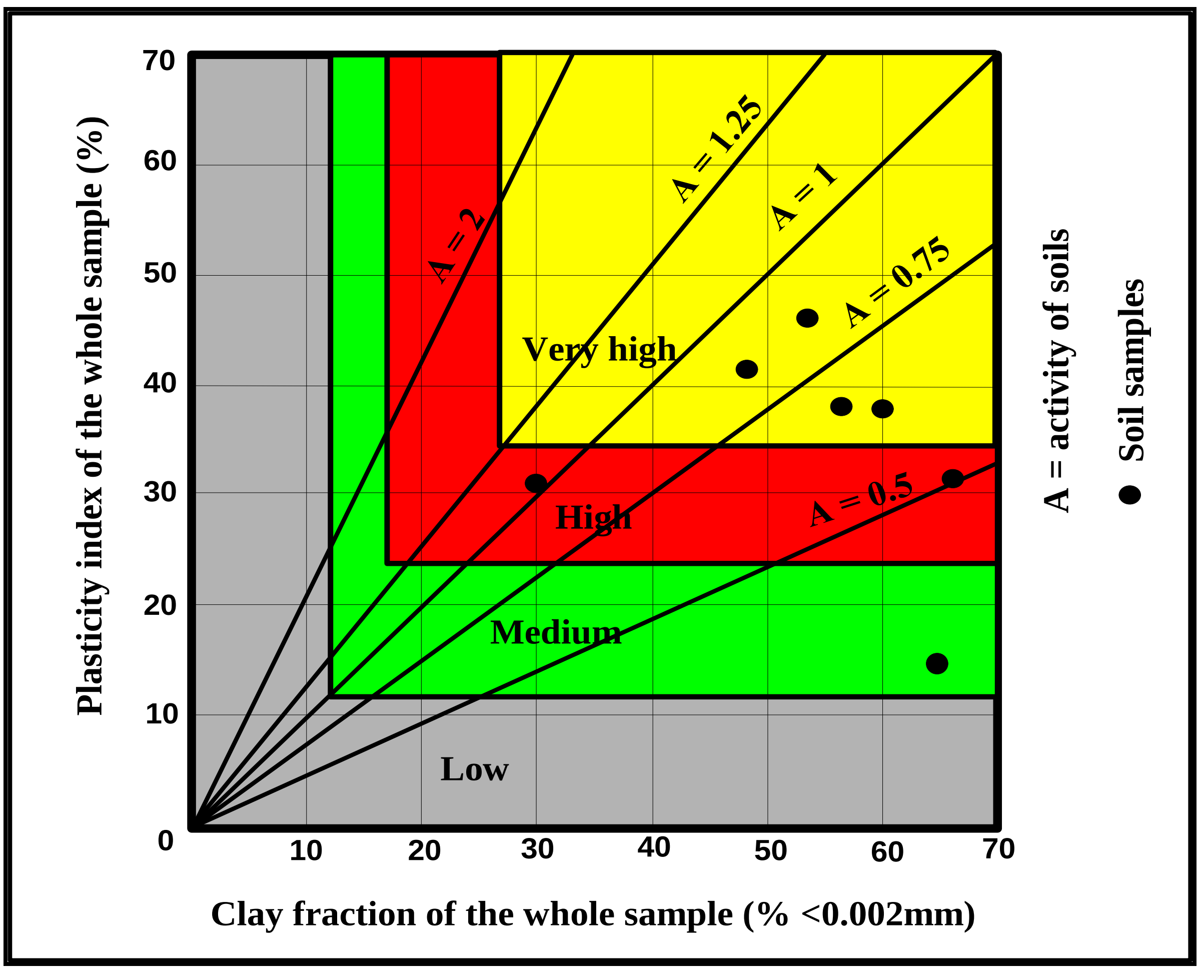

Figure 5.11 Swell potential and activity soils of the study area.

Based on the Figure 5.11, among seven soil samples four are in very high, two in high and one in medium expansiveness. Therefore, the results obtained from the direct and indirect measurements of swell potential of soils of the area are characterized by high expansiveness nature which is unfavorable for the building foundations.

The activity of soils of the study area was determined from the plasticity index (Table 5.3) and grain size analysis (Table 5.2). It was found out that the activities of soils ranges from 0.24 to 1.1. Based on the activity value, three samples are in the normal soil zone whereas the four samples placed inactive soil zone.

5.4.3 Standard Penetration Test (SPT)

Standard penetration test is important to understand strength of soils and to show a relationship with other soil properties. The N value of soils in the project site ranges from 13 to 22 (Table 5.4). Based on the standard correlation soils of the study area are characterized as stiff to very stiff with approximate compressive strength value varying from 48 to 190KN/m^2.

5.4.4 Classification of soils

For this study, the Unified Soil Classification System (USCS) and classification system proposed by IAEG (1981) which is a modified form of the Unified Soil Classification (USC) were used to classify soils of the project site. Both systems of classifications are based on the grain size and Atterberg limits of soils. Soils of the study are fine grained soils. The engineering properties of fine grain soils are mainly depend on the Atterberg limits rather than the grain size. Because of this, the classification was done based on the liquid limit and plasticity index. This systems of classification helps to understand the plasticity nature of soils and to identify the soil type.

The soils of the project site are plotted on the Casagrande plasticity chart as shown in the Figure 5.12. All soil samples fall in the high plasticity range. Based on the Unified Soil Classification System of soils of the area are silts with high plasticity nature.

Table 5.4 Standard Penetration Test (SPT) of soils of the project site.

BH No	Depth (m)	Description of soil types	N value	Relative conditions of soils.	Approximate compressive strength (cohesion) in KN/m2
2	2.6	Very dense, reddish sandy silt	20	Very stiff	96 – 190
3	3	Medium dense, yellowish silty sand	13	Stiff	48 – 96
3	7	Silty clay	25	Very stiff	96 – 190
4	3.5	Stiff, plastic greyish silty clay	13	Stiff	48 – 96
4	6	Dense to very dense, reddish to yellowish sandy silt with some clay	22	Very stiff	96 – 190
4	8	Dense to very dense, reddish to yellowish sandy silt with some clay	20	Very stiff	96 – 190
5	2.4	Dark expansive clay	17	Very stiff	96 – 190
6	2.5	Stiff, Plastic, greyish silty clay	15	Very stiff	96 – 190

Soils of the study area were plotted on plasticity chart based on IAEG (Figure 5.13). Most of the soil samples of the area are in the very high plasticity range, except two samples which fall in high and extremely high plasticity.

From both systems of classifications, all soil samples are below A Line that implies soils of the project site are silt/organic silt. The organic content of the soils of the area ranges from 13.6 to 27.51%. According to Arora (1997), silt/organic silt soils with high plasticity have high compressibility, poor workability and poor shear strength. Therefore, soils of the project site are not suitable for building foundation, because soils with high compressibility are responsible for the development of cracks and uneven settlement in the foundation part.

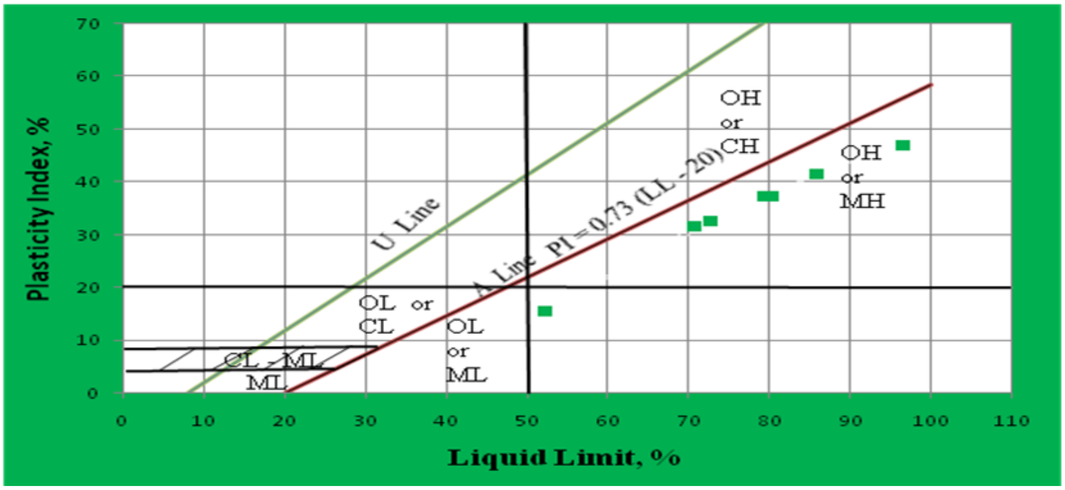

Figure 5.12 Distribution of the soils of the project site on the Casagrande plasticity chart.

5.5 Engineering properties of rocks

In this study due to the lack of elaborate data on the engineering properties of the rocks in the study area, their characterization is only based on lithological description and rock quality designation. The whole study area is covered by recent sediment deposits, but the surrounding area is covered by basalts associated with scoria. Based on the data obtained from the boreholes and surface geological map, the rocks below the sediments are basalts associated with scoria. It is characterized by highly weathered, fractured and texturally vesicular and scoracious type.

5.5.1 Rock Quality Designation (RQD)

The RQD value of rocks in the study area ranges from 65 to 100. As simple as the procedure, it has been found that there is a reasonably good relationship between the numerical values of the RQD and the general quality of the rock for engineering purposes. Based on standard description of RQD, rocks of the study area are grouped under fair, good and excellent as shown in the Table 5.5.

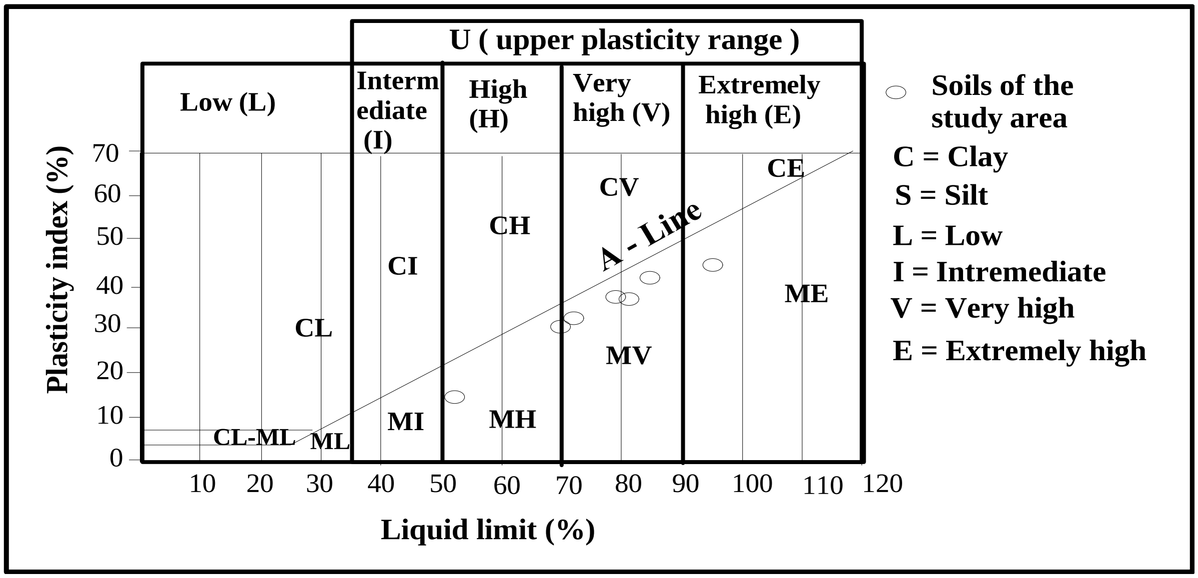

Figure 5.13 Plots of soils of the study area on plasticity chart based on IAEG.

Table 5.5 Rock Quality Designation (RQD) of the study area.

BH No	Depth (m)	Lithological description	RQD	Description of RQD
8	9	Greyish, slightly weathered basalt	65	Fair
8	10	Greyish, slightly weathered basalt	75	Good
1	8	Greyish, slightly weathered basalt	65	Fair
1	10	Greyish, slightly weathered basalt	75	Good
2	5.4	Greyish, slightly weathered vesicular basalt	60	Fair
2	8.2	Greyish, slightly weathered vesicular basalt	65	Fair
5	8.5	Reddish and greyish scoracious basalt	90	Excellent
7	6.6	Greyish, slightly weathered basalt	90	Excellent
7	8.3	Greyish, slightly weathered basalt	100	Excellent

CHAPTER SIX

CONCLUSIONS AND RECOMMENDATIONS

6.1 General

An integrated study involving geophysical and geotechnical investigation were carried out at the construction site of the Addis Ababa Science and Technology University campus located in Akaki area, southeast of Addis Ababa. The geophysical surveys included 2D electrical imaging and magnetic surveys were conducted. Some assessments were also made in relation to the seismicity of the area and its possible effect on the local construction site conditions. The geotechnical investigations included close examination of the excavated sections on the construction site, drilling results from a number of geotechnical boreholes sunk over the area and laboratory tests of soil properties and rock characteristics determinations in the field.

In the above Chapters of this thesis work, the survey profiles, the instruments employed techniques of data acquisition, interpretation of the results of those different techniques and their relevance to the foundation under construction has been examined. In this chapter we present the summary of this work and give some concluding remarks about the work. A final section gives some recommendations for the foundation work being currently undertaken based of those results.

6.2 Conclusions

Based on the geological information from the boreholes and profiles of the 2D electrical resistivity imaging surveys, vertical geological section of study area were made, which enabled to classify the subsurface into three geological layers. The top layer is recent sediment deposits, which is composed of dark expansive clay, silty clay/ clayey silt, sandy silt and granular materials. The thickness of this layer is increasing from southeast to northwest and varies from 4 to 15 m.

The second layer comprises of, highly to completely weathered and fractured, scoracious basalt and scoria. General thickness of this layer varies from 3 to 10 m, but on Profile-2 and Profile-3 it is greater than 26m in areas where the weak zone are present. The morphology of the layer is undulating and bends to depths in areas where the weak zones are found.

The third layer is slightly weathered and fresh scoracious basalt and scoria. It represents the bedrock in the study area and characterized by increment of depth from southeast to northwest direction with undulating morphology. The bedrock was a single unified block which was lately broken apart into a number of blocks due to the tectonic actvities. From a combination of the magnetic and 2D electrical resistivity imaging profiles, a number of fractures were mapped that could be interpreted as faults which have significantly influence on building foundations. Further, the results obtained from the combination of the 2D electrical resistivity imaging profiles shows that some structures are continues whereas some of the structures are localized. From this the building will be preferably construct in the northwestern side of the profile-1and 3, and southeastern side of the Profile-1 where there are few weak zones.

When one sees the four profiles side by side, depth to the bedrock is relatively shallow on Profile-3. Based on the 2D electrical resistivity imaging profiles and stacked resistivity pseudo-section map, depth to bedrock is relatively shallow at the southwestern, western, and southern part of the study are, as a result, those parts of the study area are better for building foundations.

The magnetic profiles remarkably coincide with the 2D electrical resistivity profiles in mapping the weak zones. The high magnetic anomaly response is probably due to the result of highly magnetized volcanic rocks that could be found in the area. The higher the magnetic response the shallower the fresh volcanic rocks are believed to be the bedrocks in the area. The intermediate and low magnetic anomalies are the responses of different degree of fracturing of the volcanic rocks and regions around the weak zones.

As the study area is located in the western margin of Main Ethiopia Rift which is tectonically active with intense fracturing, the suitability of the site for construction purposes can be examined from many angles one of which is its susceptibility for natural hazards like seismic activities. The possible seismic source zones are very near to the study area. The geology of the project site is covered by recent loose sediments and overlies the volcanic rocks with intense fractures. These sediments and fractures have an ability to amplify the amplitude of the waves. Because of these reasons even small magnitude of earthquake might damage the building structures easily.

The depth of water table in the area is 24m which has no significant influcence on the building foundations particularly on shallow foundations.

Several conclusions can be drawn from the direct geotechnical investigations. Grain size analysis results revealed that soils of the study area are mainly dominated by silt and clay size particles with some sand grains. The grain size analysis curves show that a missing of particle size of soils which implies that the soils of the project site is not well graded.

Generally the soils have plastic nature. Most soils of the area fall in the very high plasticity, except two which are lie in high and extremely plasticity. The result obtained from direct and indirect methods of measurements, soils of the area have very high swell of potential which is unfavorable for the building foundations. Using plasticity chart, soils of the area are classified in MH, MV and ME soil zones. According to Arora (1997), silt/organic silt soils with high plasticity are characterized by high compressibility, poor workability and shear strength. Therefore, soils of the area are not suitable for building foundation.

The N value of soils of the project site are correlated to standard descriptions and grouped under stiff to very stiff. Rocks of the area are basalts associated scoria and characterized by highly weathered and fractured, vesicular and scoracious type. Based on standard description of RQD, rocks of the area are grouped under fair, good and excellent.

6.2 Recommendations

Based on the outcomes of this study, the following recommendations are made in relation to the foundation work being currently undertaken in the area:

- Removal of undesirable soils (to depths of 3-4 m) from the foundation area and backfilling it with non compressible soils (well compacted granular soils).
- Localized zones within the survey site where the structures and prominent zones of weakness are identified. These areas need special design considerations.
- Buildings should preferably be constructed in the southwestern, southern and western part of the study area particularly in the northwestern side of the profile-1and 3 and southeastern side of the Profile-1 where the sediment thicknesses are relatively shallow and with few weak zones.
- In the north, northeastern and eastern parts of the study area, the thickness of sediments are thicker compared to the other areas. Therefore, the foundations should be extending down to the sound bedrock especially for multi- story buildings and heavy structures.
- Proper consideration of seismicity of the study area is important in the design of the foundations and superstructures due to the proximity of the area to the rift margins and the presence of weak zones mapped in the area.
- The current study covered only partial part of the university. So, additional investigation will be required for the future expansion of buildings.

References

1. Addis Ababa University, Department of Geology and Geophysics and Addis Ababa Water and Sewerage Authority (2003). Groundwater vulnerability mapping of the Addis Ababa water supply aquifers. Addis Ababa, Ethiopia, Unpublished Report.
2. Anteneh Girma (1994). Hydrogeology of Akaki Area. Addis Ababa University, Addis Ababa, Ethiopia, Unpublished Master Thesis.
3. Arora, K.R. (1997). Soil mechanics and foundation engineering, standard publisher's distributors, Delhi, India.
4. Aubert, M. (1984). Resistivity and magnetic surveys in ground-water prospecting in volcanic areas. Case history Maar of Beanit, Puy de Dome, France *Geophys. Prospect.* **32:** 63–554.
5. Benson, R.C. (1993). Geophysical Techniques for Subsurface Site Characterization. Chapter 14, In: Geotechnical Practice for Waste Disposal, David Daniel, Ed., Chapman and Hall, pp. 311-357.
6. Construction Design Share Company (2011). Geotechnical investigation report of Addis Ababa science and Technology University. Addis Ababa, Ethiopia, Unpublished Report.
7. Bowles, J. E. (1992). Engineering properties of Soils and their measurement. 4th ed., McGraw- Hill, Inc., USA, 241 pp.
8. Carrara, E. (2001). Resistivity and radar surverys at the archaeological site of Ercolano. *J. Environ. Eng. Geophys*. **6**: 32–123.
9. Daniels, F. and Alberty, R.A. (1966). Physical chemistry. New York: John Wiley and Sons Inc.
10. Davis, S. N. and DeWiest, R.J.M. (1996). Hydrogeology. John Wiley and sons Inc. New York, 463 pp.
11. Deere, D U. (1967). Design of surface and near surface constructions in rock. Proc. 8th U.S. Symp. Rock Mechanics, ed. Fairhurst, publ. AIME, New York, PP. 237-300.
12. DeGroot-Hedlin, C. and Constable, S. (1990). Occam's inversion to generate smooth, two dimensional models form magneto telluric data. *Geophysics*, **55**:1613-1624.
13. Ebasa Alijira (2006). Numerical Groundwater flow simulation of Akaki River Catchment. Addis Ababa University, Addis Ababa, Ethiopia, Unpublished Master Thesis.

14. Ethiopian Building Code Standard (1995). Code of Standards for Seismic Loads. Ministry of Works and Urban Development, Addis Ababa, Ethiopia.
15. Geotomo Software (2006). RES2DINV Ver. 3.55, Rapid 2-D Resistivity and IP inversion using the least-squares method (available at www.geoelectrical.com).
16. Getech (2007). Advanced Processing and Interpretation of Gravity and Magnetic Data (available at http: //www.getech.com.).
17. Griffiths, D.H. and Barker, R.D. (1993). Two-dimensional resistivity imaging and modelling in areas of complex geology. *Journal of Applied Geophysics*, **29**: 211-226.
18. Haile Sellasie Girmay and Getaneh Assefa (1989). The Addis Ababa-Nazareth Volcanics: A Miocene-Pleistocene Volcanic Succession in Ethiopian Rift. *SINET: Ethiopian Journal of Science*, **12**(1).
19. Holtz, W.G. and Gibbs, H.J. (1956). Engineering Properties of Expansive Clays. Trans ASCE. 121 pp.
20. Holtz, R.D and Kovacs, W.D. (1981). An introduction to geotechnical engineering prentice- Hall, Inc., Englewood Cliffs, New Jersey, 719 pp.
21. International Association of Engineering Geologist (1981). Rock and Soil Description and Classification for Engineering Geological Mapping. Report by IAEG Commission on Engineering Geological Mapping. *Bull. Int. Assoc. Eng. Geol.*, **24**: 235-274.
22. Keller, G.V. and Frischknecht, F.C. (1966). Electrical Methods in Geophysical Prospecting. Pergamon Press, Oxford, 519 pp.
23. Kunetz, G. (1996). Principles of direct current resistivity prospecting. Gebruder-Borntrager, Berlin- Nikolassee, 103 pp.
24. Loke, M.H. (1997). Electrical imaging surveys for environmental and engineering studies: a practical guide to 2D and 3D surveys: Unpublished short training course lecture notes, University of Sains Malaysia, Penang, Malaysia.
25. Loke, M.H. (1999). Electrical imaging surveys for environmental and engineering studies. A practical guide to 2-D and 3-D surveys, Penang, Malaysia, 57 pp.
26. Lowrie, W. (2007). Fundamentals of Geophysics Second Edition Cambridge, New York, pp. 282 - 360
27. Morton, W.H. (1979). Riftward Younging of Volcanic Rocks in the Addis Ababa Region. Rift Valley Ethiopian. *Nature*, **280**: 284 – 288.

28. Murthy, V.N.S. (2002). Geotechnical engineering: principles and practices of soil mechanics and foundation engineering, Marcel Dekker, Inc. New York, 1028 pp.
29. Raghuvanshi, T.K. (2010). Lecture Notes: Geotechnical Investigation, Addis Ababa University, Ethiopia.
30. Reynolds, J.M. (1997). An Introduction to Applied and Environmental Geophysics. John Wiley and Sons limited, England, UK. pp. 116-209, 415-522.
31. Rivas, J.E. (2009). Geothermal training programme: gravity and magnetic methods Ahuachapán and Santa Tecla, El Salvador, United Nations University, 13 pp.
32. Sasaki, Y. (1992). Resolution of resistivity tomography inferred from numerical simulation. *Geophys Prospect*, **40**: 453–46.
33. Seed, H.B. (1960). The strength of compacted cohesive soils. *Proceedings*, ASCE Research Conference on Cohesive Soils, Boulder, pp. 877-964.
34. Singh, S.K. (1997). Dynamic deformation of shallow sediments in the valley of Mexico, part II: Single station estimates. *Bull. Seismol. Am*. **87.** 540-550.
35. Skempton, A. W. (1953). The colloidal activity of clays. *In* Proceedings of the Third International Conference on Soil Mechanics and Foundation Engineering: Zurich, Switzerland, ICOSOMEF, **1:** 57-61.
36. Skempton, A. W. (1986). Standard Penetration Test Procedures and the effects on sand of overburden pressure, relative density, particle size and over consolidation. Geotechnical, 36 (3): 425-447.
37. Soupios, P. (2007). Reconstructing former urban environments by combining geophysical electrical methods and geotechnical investigations. *Geophys. Eng.* **5**: 186 –194.
38. Thomas, M.B. (2003). Introduction to geophysical exploration: magnetic notes on main magnetic field (available at galitzin.mines.edu/…/notes).
39. Tigistu Haile (2010). Applications of electrical resistivity tomography (at www.mawari.net.).
40. Tilahun Mammo (2005). Site-specific ground motion simulation and seismic response analysis at the proposed bridge sites within the city of Addis Ababa, Ethiopia. *Engineering Geology*, **79**: 127–150.
41. Van Der Merwe, D.H. (1964). The Prediction of Heave from the Plasticity Index and Percentage clay Fraction of Soils. Civil Engineer in South Africa, **6** (6): 103-106.

42. Zanettin, B. and Justin V. E. (1974). The Volcanics of Western Afar and Ethiopian Rift Margins. Padova, Italy, **9**: 567–574.

APPENDIX-1

Table1: Lithological log of the study area (after CDSC, 2011)

Location X: 478935 Y: 981802	Description of strata with depth	Location X: 479192 Y: 982048	Description of strata with depth	Location X:479184 Y: 982308	Description of strata with depth
0 – 0.60 m	Dark expansive clay	0 – 1.50 m	Dark expansive clay	0 – 1.50 m	Dark expansive clay
0.60 m – 3.10 m	Fractured and highly weathered scoria	1.50 m – 2.60 m	Stiff, grayish silty clay/ clayey silt	1.50 m – 3.00 m	Highly to completely weathered rock
3.10 m – 10.00 m	Slightly weathered scoria	2.60 m – 4.00 m	Very dense, reddish sandy silt	3.00 m – 5.00 m	Medium dense, yellowish silty sand
		4.00 m – 8.20 m	Grayish, slightly weathered scoracious basalts	5.00 m – 7.60 m	Highly to completely weathered rock
		8.20 m – 9.20 m	highly to completely weathered scoracious basalt	7.60 m – 10.00 m	Reddish, highly weathered and fractured scoria

BH 1

BH 2

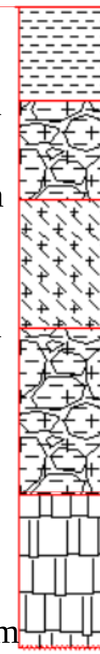

BH 3

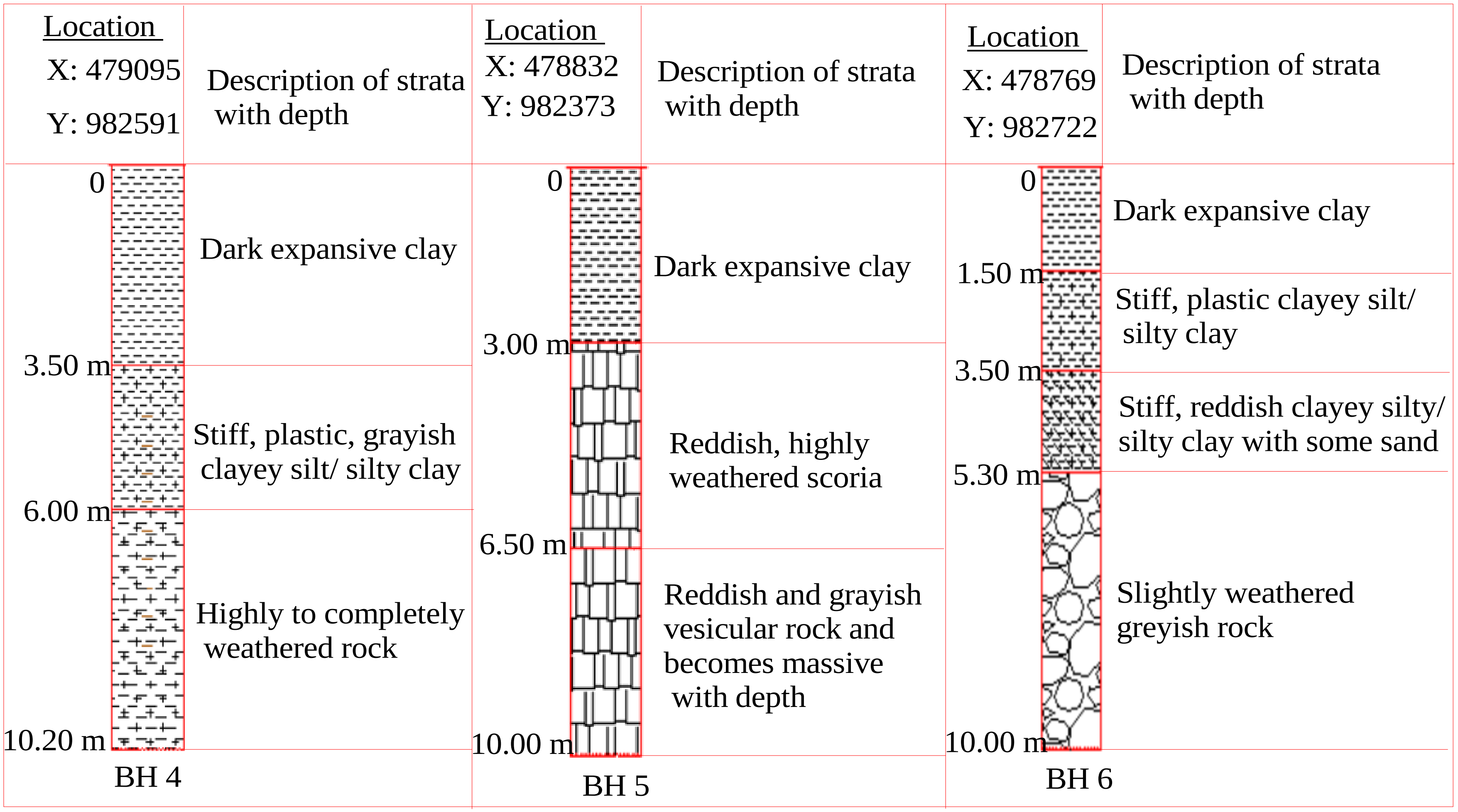

Location
X: 479095
Y: 982591
Description of strata with depth
0
Dark expansive clay
3.50 m
Stiff, plastic, grayish clayey silt/ silty clay
6.00 m
Highly to completely weathered rock
10.20 m
BH 4
Location
X: 478832
Y: 982373
Description of strata with depth
0
Dark expansive clay
3.00 m
Reddish, highly weathered scoria
6.50 m
Reddish and grayish vesicular rock and becomes massive with depth
10.00 m
BH 5
Location
X: 478769
Y: 982722
Description of strata with depth
0
Dark expansive clay
1.50 m
Stiff, plastic clayey silt/ silty clay
3.50 m
Stiff, reddish clayey silty/ silty clay with some sand
5.30 m
Slightly weathered greyish rock
10.00 m
BH 6

Location x: 478560 y: 982504	Description of strata with depth
0 – 1.5 m	Dark expansive clay
1.5 m – 4.00 m	Highly weathered and fractured basalt
4.00 m – 10.00 m	Greyish, slightly weathered basalt
BH 7	

Location x: 478575 y: 982064	Description of strata with depth
0 – 0.7 m	Dark, expansive clay
0.7 m – 7.00 m	Highly weathered and fractured basalt
7.00 m – 10.00 m	Grayish, slightly weathered basalt
BH 8	

APPENDEX-2

Table 2: Magnetic susceptibilities and Resistivities of some common rocks, soils, water and minerals.

Mineral or rock types	Susceptibility (k) (rationalized SI units)	Mineral or rock types	Resistivity (ohm- m)
Dolomite (pure)	-12.5 to 44	Igneous and Metamorphic Rocks	
Dolomite (impure)	20,000	Granite	$5x10^3$-10^6
Limestone	10 to 25,000	Basalt	10^3-10^6
Sandstone	0 to 21,000	Slate	$6x10^2$-$4x10^7$
Shale	60 to 18,600	Marble	10^2-$2.5x10^8$
Schist	315 to 3000	Quartzite	10^2-$2x10^8$
Slate	0 to 38,000	Sedimentary Rocks	
Gneiss	125 to 25,000	Sandstone	8-$4x10^3$
Serpentenite	3,100 to 75,000	Shale	20-$2x10^3$
Granite	20 to 50,000	Limestone	50-$4x10^2$
Rhyolites	250 to 37,7000	Soils and waters	
Pegmatite	3,000 to 75,000	Clay	1-1000
Gabbro	800 to 76,000	Alluvium	10-800
Basalts	5000 to 182,000	Groundwater (fresh)	10-100
Oceanic Basalts	300 to 3,6000	Sea water	0.2
Perdotite	95,000 to 196,000		

APPENDIX-3

Table 3: Grain size analysis

soil samples	1	2	3	4	5	6	7
Sieve Size (mm)	Percent Passing (%)	Percent Passing (%)	Percent Passing (%)	Percent Passing (%)	Percent Passing (%)	Percent Passing (%)	Percent Passing (%)
75	100.00	100.00	100.00	100.00	100.00	100.00	100.00
63	100.00	100.00	100.00	100.00	100.00	100.00	100.00
50	100.00	100.00	100.00	100.00	100.00	100.00	100.00
37.5	100.00	100.00	100.00	100.00	100.00	100.00	100.00
25	100.00	100.00	100.00	100.00	100.00	100.00	100.00
19	100.00	100.00	100.00	100.00	100.00	100.00	100.00
12.5	100.00	100.00	100.00	100.00	100.00	100.00	100.00
9.5	100.00	100.00	100.00	100.00	100.00	100.00	100.00
4.75	100.00	100.00	100.00	100.00	100.00	100.00	100.00
2	100.00	100.00	100.00	100.00	100.00	100.00	100.00
1.18	100.00	100.00	100.00	98.00	100.00	100.00	100.00
0.6	99.76	99.76	99.18	93.82	100.00	99.52	99.62
0.3	99.38	99.44	99.08	90.78	99.40	98.88	99.36
0.15	99.00	98.70	98.68	87.68	98.22	97.88	98.74
0.075	98.50	97.90	98.52	85.28	97.08	96.82	98.08
0.032	77.72	84.48	87.86	60.83	87.86	77.72	70.97
0.021	74.34	81.10	84.48	57.45	84.48	74.34	67.59
0.012	70.97	77.72	81.10	54.07	81.10	70.97	67.59
0.009	67.59	74.34	77.72	47.31	77.72	67.59	64.21
0.006	64.21	70.97	74.34	40.55	74.34	64.21	64.21
0.003	54.07	64.21	67.59	33.79	67.59	60.83	57.45
0.001	43.93	54.07	57.45	27.03	57.45	54.07	50.69

Table 4: Standard penetration test N- values in cohesive and granular soils

SPT–N Cohesive soils	Relative conditions of soils	Approximate compressive strength	SPT –N of Granular soils	Relative conditions of soils	Relative density (%)
2 – 4	Soft	12-24	0-4	Very loose	0-15
4 – 8	Medium	24-48	4-10	Loose	15-35
8 – 15	Stiff	48-96	10-30	Medium	35-65
15 – 30	Very stiff	96-190	30-50	Dense	65-85
>30	Hard	>190	>50	Very dense	85-100

Table 5: Soil classifications according to Plasticity Index

Plasticity index	Plasticity
0	Non-plastic
<7	Low plastic
7-17	Medium plastic
>17	Highly plastic

Table 6: General engineering suitability of the soils (Arora, K, R, 1997)

Soil Group		Permeability	Compressibility	Shear Strength	Workability
Gravels	GW	Pervious	Negligible	Excellent	Excellent
	GP	Very pervious	Negligible	Good	Good
	GM	Semi-Pervious to Impervious	Negligible	Good	Good
	GC	Impervious	Very Low	Good to fair	Good
Sands	SW	Pervious	Negligible	Excellent	Excellent
	SP	Pervious	Very low	Good	Fair
	SM	Semi-Pervious to impervious	Low	Good	Fair
	SC	Pervious	Low	Good to fair	Good
Low and medium plasticity silt and clays	ML,MI	Semi-Pervious to impervious	Medium	Fair	Fair
	ML, CI	Impervious	Medium	Fair	Good to Fair
	OL, OI	Semi-Pervious to impervious	Medium	Fair	Fair
High plasticity silts and clays	MH	Semi-Pervious to impervious	High	Fair to Poor	Poor
	CH	Impervious	High	Poor	Poor
	OH	Impervious	High	Poor	Poor